Springer

Dear Author

Here are the proofs of your article.

- You can submit your corrections **online** or by **fax**.
- For **online** submission please insert your corrections in the online correction form. Always indicate the line number to which the correction refers.
- Please return your proof together with the permission to publish confirmation.
- For **fax** submission, please ensure that your corrections are clearly legible. Use a fine black pen and write the correction in the margin, not too close to the edge of the page.
- Remember to note the journal title, article number, and your name when sending your response via e-mail, fax or regular mail.
- **Check** the metadata sheet to make sure that the header information, especially author names and the corresponding affiliations are correctly shown.
- **Check** the questions that may have arisen during copy editing and insert your answers/corrections.
- **Check** that the text is complete and that all figures, tables and their legends are included. Also check the accuracy of special characters, equations, and electronic supplementary material if applicable. If necessary refer to the *Edited manuscript*.
- The publication of inaccurate data such as dosages and units can have serious consequences. Please take particular care that all such details are correct.
- Please **do not** make changes that involve only matters of style. We have generally introduced forms that follow the journal's style.
  Substantial changes in content, e.g., new results, corrected values, title and authorship are not allowed without the approval of the responsible editor. In such a case, please contact the Editorial Office and return his/her consent together with the proof.
- If we do not receive your corrections **within 48 hours**, we will send you a reminder.

Please note

Your article will be published **Online First** approximately one week after receipt of your corrected proofs. This is the **official first publication** citable with the DOI. **Further changes are, therefore, not possible.**

After online publication, subscribers (personal/institutional) to this journal will have access to the complete article via the DOI using the URL:

`http://dx.doi.org/10.1007/s11042-020-09831-4`

If you would like to know when your article has been published online, take advantage of our free alert service. For registration and further information, go to: http://www.springerlink.com.

Due to the electronic nature of the procedure, the manuscript and the original figures will only be returned to you on special request. When you return your corrections, please inform us, if you would like to have these documents returned.

The **printed version** will follow in a forthcoming issue.

AUTHOR'S PROOF

Metadata of the article that will be visualized in OnlineFirst

Article Title	**Gravitational search algorithm: a comprehensive analysis of recent variants**	
Article Sub- Title		
Article Copyright - Year	**Springer Science+Business Media, LLC, part of Springer Nature 2020 (This will be the copyright line in the final PDF)**	
Journal Name	Multimedia Tools and Applications	
Corresponding Author	Family Name	**Tripathi**
	Particle	
	Given Name	**Ashish**
	Suffix	
	Organization	Malaviya National Institute of Technology
	Division	
	Address	Noida, India
	e-mail	mail2ashish07@gmail.com
Author	Family Name	**Mittal**
	Particle	
	Given Name	**Himanshu**
	Suffix	
	Organization	Malaviya National Institute of Technology
	Division	
	Address	Noida, India
	e-mail	
Author	Family Name	**Pandey**
	Particle	
	Given Name	**Avinash Chandra**
	Suffix	
	Organization	Malaviya National Institute of Technology
	Division	
	Address	Noida, India
	e-mail	
Author	Family Name	**Pal**
	Particle	
	Given Name	**Raju**

32 Suffix
33 Organization: Malaviya National Institute of Technology
34 Division
35 Address: Noida, India
36 e-mail

37 Schedule — Received: 23 January 2020
38 Revised: 14 August 2020
39 Accepted: 9 September 2020

40 Abstract

Gravitational search algorithm is a nature-inspired algorithm based on the mathematical modelling of the Newton’s law of gravity and motion. In a decade, researchers have presented many variants of gravitational search algorithm by modifying its parameters to efficiently solve complex optimization problems. This paper conducts a comparative analysis among ten variants of gravitational search algorithm which modify three parameters, namely *Kbest*, velocity, and position. Experiments are conducted on two sets of benchmark categories, namely standard functions and CEC2015 functions, including problems belonging to different categories such as unimodal, multimodal, and unconstrained optimization functions. The performance comparison is evaluated and statistically validated in terms of mean fitness value and convergence graph. In experiments, IGSA has achieved better precision with balanced trade-off between exploration and exploitation. Moreover, triple negative breast cancer dataset has been considered to analysis the performance of GSA variants for the nuclei segmentation. The variants performance has been analysed in terms of both qualitative and quantitive with aggregated Jaccard index as performance measure. Experiments affirm that IGSA-based method has outperformed other methods.

41 Keywords separated by ' - ': Optimization algorithm - Nature-inspired algorithm - Gravitational search algorithm

Multimedia Tools and Applications
https://doi.org/10.1007/s11042-020-09831-4

Gravitational search algorithm: a comprehensive analysis of recent variants

Q1 Himanshu Mittal[1] · Ashish Tripathi[1] · Avinash Chandra Pandey[1] · Raju Pal[1]

Received: 23 January 2020 / Revised: 14 August 2020 / Accepted: 9 September 2020

Abstract

Gravitational search algorithm is a nature-inspired algorithm based on the mathematical modelling of the Newton's law of gravity and motion. In a decade, researchers have presented many variants of gravitational search algorithm by modifying its parameters to efficiently solve complex optimization problems. This paper conducts a comparative analysis among ten variants of gravitational search algorithm which modify three parameters, namely $Kbest$, velocity, and position. Experiments are conducted on two sets of benchmark categories, namely standard functions and CEC2015 functions, including problems belonging to different categories such as unimodal, multimodal, and unconstrained optimization functions. The performance comparison is evaluated and statistically validated in terms of mean fitness value and convergence graph. In experiments, IGSA has achieved better precision with balanced trade-off between exploration and exploitation. Moreover, triple negative breast cancer dataset has been considered to analysis the performance of GSA variants for the nuclei segmentation. The variants performance has been analysed in terms of both qualitative and quantitive with aggregated Jaccard index as performance measure. Experiments affirm that IGSA-based method has outperformed other methods.

Keywords Optimization algorithm · Nature-inspired algorithm · Gravitational search algorithm

1 Introduction

Generally, optimization problems are the set of problems which are quite complex and difficult to solve, especially when defined in high-dimensional space. On some instances, such problems could not be mathematically formulated due to incomplete information. On these problems, traditional deterministic algorithms cannot provide sophisticated solutions. Therefore, nature-inspired algorithms [6] are used to solve such types of optimization problems. Over the last twenty years, nature-inspired algorithms have been quite successful, especially on nonlinear real-world optimization problems [7, 37]. In general, nature-inspired

✉ Ashish Tripathi
mail2ashish07@gmail.com

1 Malaviya National Institute of Technology, Noida, India

algorithm is a mathematical model that imitates the optimization characteristics of a natural system and generates an optimal solution [12]. A detailed review of nature-inspired algorithms along with their mathematical proofs have been discussed by Nayyar et al. [39]. Additionally, Nayya and Nguyen [40] discussed adaptability and diversity along with issues and future of these algorithms. Nayyar et al. [38] list out some of the popular nature-inspired algorithms. Genetic algorithm [61], differential algorithm [55], particle swarm optimization [17], ant colony optimization [8], biogeography-based optimizer [54], and artificial bee colony [15] are names of some popular nature-inspired algorithms. However, there are many other phenomena in nature that may be considered for solving other types of real-world problems. Newton's law of gravity and motion is one of such phenomena, which inspired Rashedi et al. [46] to introduce a new nature-inspired algorithm, termed as gravitational search algorithm (GSA).

GSA is one of the well-known nature-inspired algorithms which has shown robust performance on numerous real-world problems like parameter selection, image segmentation, energy conservation, and networking [28, 33, 34]. A survey of various applicabilities of GSA have been studied in [48]. The unique attribute of GSA is the inclusion of Newtonian laws of gravity for the solution updation which makes it a stable algorithm too. Moreover, it doesn't memorize solutions to obtain optimal solution and therefore, it is a memory-less algorithm [42]. However, there are number of demerits in GSA such as poor solution precision, trapping into local optima, and poor convergence rate [48]. To mitigate these, a number of GSA variants have been proposed in literature. Thus, this paper provides an extensive analyses of these existing variants of GSA.

In GSA, the trade-off between exploration and exploitation is regulated through $Kbest$ function which defines 'K' number of best solutions that apply gravitational force in an iteration. Generally, this function decreases linearly with increasing iterations and thus, GSA has a linear transition from exploration to exploitation [58]. However, this linear transition results in reduced exploration at later iterations which increases the probability of trapping into local optimum [50, 59]. Additionally, another influential parameters which effect the performance of GSA are velocity and position. Literature has signified that modification of the velocity and position equations have enhanced the convergence rate and improved diversity in the search space, respectively [48]. These parameters have resulted in better solution precision and robustness. Thus, researchers have proposed various variants of GSA by modifying the position, velocity, and $Kbest$. Worth to mention that these variants of GSA have helped researchers to tackle challenging real-world problems [48]. However, there is no research article which has compared GSA variants based on these three parameters. Therefore, this paper makes following contributions.

- In this paper, nine variants of GSA are studied, each modifies one of the three parameters, namely $Kbest$, velocity, and position.
- These varaints are compared against seven recent nature-inspired algorithms along with GSA.
- In experimentation, extensive analysis have been performed through 17 standard and 28 CEC benchmark functions over four dimensional settings, i.e. 10, 30, 50, and 90.
- The experimental results are evaluated and statistically analyzed in terms of mean fitness value and convergence graph.
- The performance of the GSA varaints is evaluated in segmenting the breast cancer nuclei from histopathological images.

The organisation of the paper is as follows; Related works is discussed in Section 2 while Section 3 describes the GSA in detail. Section 4 discusses the considered variants of

GSA followed with the experimental results in Section 5. Lastly, the conclusion is drawn in Section 6.

2 Related works

In last decade, a number of variants for the GSA has been introduced in the literature to enhance its efficiency across the different domains of engineering over the non differentiable and complex optimization problems. Shaw et al. [53] developed opposition-based GSA (OGSA) which leverages the strength of opposition-based learning. Chatterjee et al. [3] introduced improved GSA using the concept of wavelet theory which has witnessed better exploration ability as compared to the parent algorithm. Similarly, Mirjalili et al. [26], induced velocity parameters in the GSA to magnify the exploitation process of the GSA. On the same footprint, Niknam et al. [41] introduced self-adaptive mutation in the GSA and developed an improved GSA algorithm. Thereafter, Mirjalili et al. [27] presented adaptive GSA (AGSA) to modify the exploitation of the GSA. Subsequently, Li et al. [21] developed piecewise GSA by changing the gravitational constant with piecewise equation. Additionally, Li et al. [20] also introduced weighted inertia mass for the objects to make faster convergence in the GSA. Davarynejad et al. [5] presented a mass-dispersed gravitational search algorithm (mDGSA) to mitigate the centre of bias characteristic of GSA.

Pelusi et al. [44] used hyperbolic sin functions based acceleration coefficients for improving the exploration and exploitation capabilities. A self-adaptive gravitational constant has been used by Lei et al. [19] to improve the low search performance and premature convergence. Giladi and Sintov [10] proposed an efficient GSA based on manifold learning for improving exploration rate. Liu et al. [23] proposed an improved gravitational algorithm with dynamically adjusting inertia weight and trend factors of speed and position. Jiang et al. [16] used chaotic gravitational constants for the gravitational search algorithm to improve the exploration ability. Guha et al. [11] used clustering technique in order to make the initial population distributed over the entire feature space and to increase the inclusion of features.

Further, Yin et al. [63] introduced CROGSA that exploits the promising knowledge extracted from the global optimal solution to improve the performance. Bansal et al. [1] proposed a fitness varying gravitational constant in GSA to control the stagnation issue. Wang et al. [60] proposed a hierarchical gravitational search algorithm with an effective gravitational constant to address the issues of premature convergence and a low search ability. Mukherjee et al. [35] presented mutation-based chaotic gravitational search algorithm to mitigate the weakness of original GSA. Rawal et al. [49] introduced fast convergent GSA that uses a sigmoidal function along with exponential step size to enhance the convergence speed and exploitation capability. A fuzzy adaptive gravitational search algorithm (FAGSA) using Tsallis entropy has been introduced to obtain the optimal 2D multilevel thresholds for image segmentation [56]. Thakur et al. [57] proposed a hybridized method based on GSA, and quantum mechanics to solve scheduling problems for multi-processor computing systems.

3 Gravitational search algorithm (GSA)

In GSA, a group of swarm agents search for an optimal solution in the collective manner. Each search agent applies the gravitational force to the other search agent. Initially, a large number of search agents are used to explore the whole search space by interacting with other and then these are converge towards the region having global optima. The searching mechanism is monitored by a $Kbest$ function. If the search space need to be explored, then the $Kbest$ value is kept larger otherwise for exploitation smaller $Kbest$ value is considered. Every search agent have a mass value associated with it. The heavier mass search agent is considered as the best solution. It means the heavier mass search agent have the better fitness values as compared to other search agents. Therefore, all other search agents are trying to move towards the heaviest mass due to the laws of gravity and motion and the heaviest solution is considered as the optimal solution for the current iteration.

Figure 1 explains the concept of the GSA with force and motion mechanism using the vector diagram. In the figure, four search agents (O_1 to O_4) are shown with different sizes. The agent with larger size is considered as heavier mass search agent and it is having better fitness value. So, in the figure, O_3 is the best solution ($gBest$) and O_4 is the worst solution ($gWorst$) for a particular iteration. The search agent O_1 updates its position value based on the force applied by other search agents (F_{12}, F_{13}, and F_{14}) on it. However, the resultant movement vector (L_1) of O_1 is shown towards O_3 due to heavy force component applied by it. Further, the mathematical formulations of the GSA method are also explained below.

Let's consider a swarm contains P search agents and each search agent has d dimensions. The i_{th} search agent (S_i) can be represented as (1).

$$S_i = (s_i^1, s_i^2, ..., s_i^d), i = 1, 2, ..., P \tag{1}$$

The updated position of search agent S_i at iteration $t+1$ is given by the (2).

$$S_i(t+1) = S_i(t) + V_i(t+1). \tag{2}$$

where, $S_i(t)$ is the search agent at iteration t and $V_i(t+1)$ is the updated velocity of i^{th} search agent and given by (3).

$$V_i(t+1) = rand \times V_i(t) + a_i(t), \tag{3}$$

Here, $a_i(t)$ is the acceleration of search agent i at t^{th} iteration and calculated as (4)

$$a_i(t) = \frac{Force_i(t)}{Mass_i(t)}, \tag{4}$$

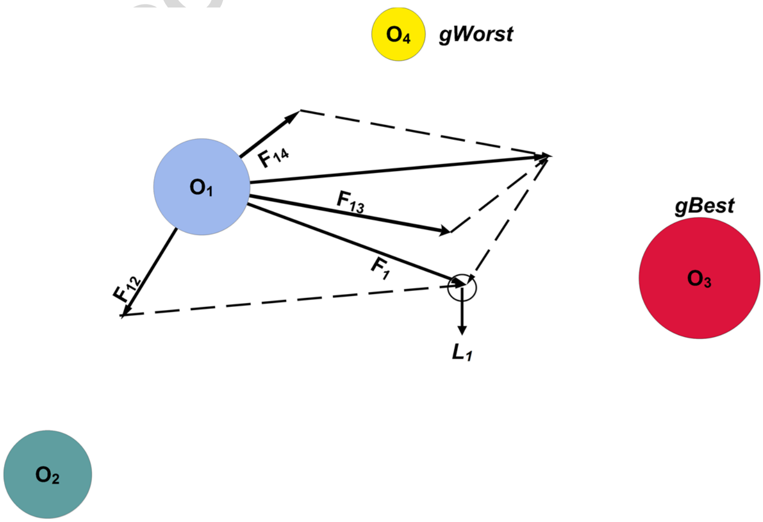

Fig. 1 Demonstration of position update in the GSA

here, $Force_i(t)$ and $Mass_i(t)$ correspond to the total force and mass of i^{th} object at t^{th} iteration respectively.

There are two types of masses of a search agent, namely inertia mass and gravitational mass. The authors of the GSA considered these masses to be equal. Therefore, the mass $Mass_i(t)$ of i^{th} search agent at t^{th} iteration is calculated as (5).

$$Mass_i(t) = \frac{m_i(t)}{\sum_{j=1}^{P} m_j(t)}, \tag{5}$$

$$m_i(t) = \frac{f_i(t) - bad(t)}{good(t) - bad(t)}, \tag{6}$$

$$good(t) = \min_{j \in \{1,\ldots,P\}} f_j(t) \tag{7}$$

$$bad(t) = \max_{j \in \{1,\ldots,P\}} f_j(t) \tag{8}$$

where, $f_i(t)$ is the i^{th} search agent fitness value, $good(t)$ and $bad(t)$ are calculated by (7) and (8) respectively for minimization problem.

Moreover, the total force $Force_i(t)$ is the weighted sum of the force applied by $Kbest$ randomly selected search agents on th search agent and it is given in (9).

$$Force_i(t) = \sum_{j=1, j\neq i}^{Kbest} rand F_{ij}(t), \tag{9}$$

where, $rand$ is a random number between 0 and 1. F_{ij} is the force of j^{th} search agent on i^{th} search agent and is calculated by (10).

$$F_{ij}{}^{r}(t) = G(t)\frac{Mass_i(t) \times Mass_j(t)}{R_{ij}(t) + \epsilon}(s_j(t) - s_i(t)) \tag{10}$$

In (9), $Kbest$ is given as (11) at t^{th} iteration.

$$Kbest(t) = final\_per + \left(\frac{1-t}{maxit}\right) \times (100 - final\_per), \tag{11}$$

where, $maxit$ is the iteration count and $final\_per$ is the percentage of search agents selected to apply force. It is observed that $Kbest$ decreases linearly over iterations as depicted in Fig. 2 which represents the behavior of $Kbest$ with the increasing number of iterations. Moreover, the step-wise procedure and flow chart of GSA are depicted in Algorithm 1 and Fig. 3, respectively.

Algorithm 1 Gravitational search algorithm (GSA) [47].

Input: Let P search agents and a gravitational constant (G_0).
Output: An optimal solution.

```
Randomly initialize the swarm having P search agents;
while stopping condition does not meet do
    Determine the fitness (f), G, and mass (Mass);
    Determine Kbest as:
    Kbest(t) = P × (final_per + (1 − t/maxit) × (100 − final_per)) / 100,
    Determine acceleration (a) and velocity (V1v)
    Updated the search agents as S(t + 1) = S(t) + V(t + 1)
end while
```

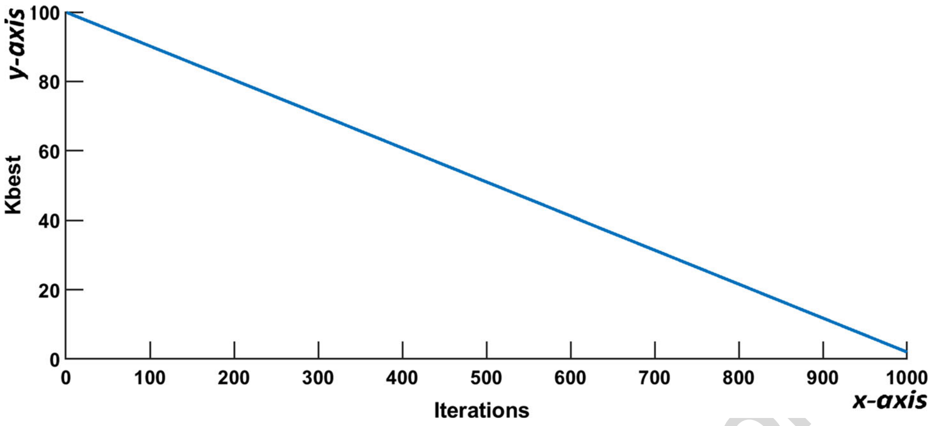

Fig. 2 $Kbest$ over iterations

4 Considered GSA variants

In literature, each GSA variant modifies atleast one parameter. In this paper, varaints based on three parameters are studied, namely position, velocity, and $Kbest$. In total, this paper compares ten variants of GSA which are detailed in following sections.

4.1 Position-based variants

In this category, three variants are considered which modifies the position equation to enchance the solution diversity.

4.1.1 Intelligent GSA (IGSA)

Mittal et al. [32] introduces IGSA in which the position parameter is modified by incorporating the position values of the global best ($gBest$) and global worst ($gWorst$) object. Equation (12) defines the modified position updation equation of i^{th} object at the t^{th} iteration.

$$x_i^d(t+1) = x_i^d(t) + v_i^d(t+1) + \underbrace{r(t) \times \frac{(gBest^d(t) - x_i^d(t))}{|(\rho \times gWorst^d(t)) - x_i^d(t))|}}_{Intelligent\ component} \tag{12}$$

where, $r(t)$ and ρ correspond to a random number and a constant. The $gBest$ adds an additive effect by moving other objects towards itself which is proportioned by $gWorst$. This advantages in better solution precision.

4.1.2 Disruption-based GSA (DGSA)

In DGSA, Sarafrazi et al. [51] introduced the disruption operator in position parameter. The modified position equation for the i^{th} individual (X_i) at $(t+1)$ iteration is formulated as (13).

$$X_i(t+1) = X_i(t).D \tag{13}$$

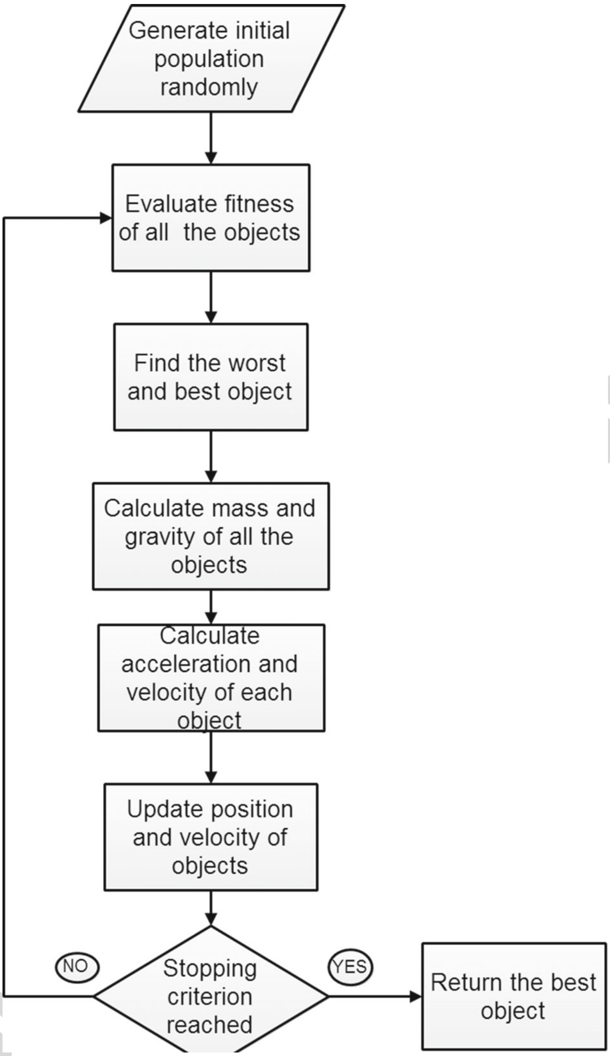

Fig. 3 Flow chart of GSA

where D is the disruption operator and equated as (14). 183

$$D = \begin{cases} R_{i,j}.U(-0.5, 0.5) & if\, R_{i,best} \geq 0 \\ 1 + \epsilon.U(-0.5, 0.5) & else \end{cases} \tag{14}$$

where, 184

$$\frac{R_{i,j}}{R_{i,best}} < \theta \left(1 - \frac{1}{t_{max}}\right) \tag{15}$$

4.1.3 Opposition-based GSA (OGSA)

Shaw et al. [53] proposed opposition-based GSA (OGSA) by incorporating the concept of opposition-based learning during the position initialization and position updation. Equation (16) generates opposite point for the x_i. The inclusion of opposite population advantages in accelerating the performance.

$$\overline{x_i} = a_i + b_i - x_i \tag{16}$$

4.2 Velocity-based variants

This includes the GSA variants which redefines the velocity equation for achiving better convergence.

4.2.1 Adaptive GSA (AGSA)

Mirjalili et al. [27] presented an adaptive GSA (AGSA) by modifying the velocity equation in which position of best object in an iteration is incorporated. The updated velocity equation is presented in (17). This benefits AGSA in achieving better exploitation.

$$V_i(t+1) = rand \times V_i(t) + c_1' \times ac_i(t) + c_2' \times (gbest - X_i(t)) \tag{17}$$

4.2.2 Modified GSA (MGSA(I))

In MGSA(I), the velocity equation is modified to control the trajectory followed by GSA. Here, Khajehzadeh et al. [18] clamped the velocity oscillation within the reasonable interval which is equated in (18).

$$-V_{max} \leq v_i^d \leq V_{max} \tag{18}$$

where, V_{max} is defined by (19).

$$V_{max} = [1 - (t/t_{max})^h] \times V_{max0} \tag{19}$$

where, V_{max0} is initalized according to (20).

$$V_{max0} = rand \times (x_{max} - x_{min}) \tag{20}$$

4.2.3 Modified GSA (MGSA(II))

In MGSA(II), Han and Chang [13] modified the velocity equation with the chaotic parameter. Equation (21) formulates the modified velocity of the i_{th} object (X_i) for the (t+1) iteration.

$$v_i^d(t+1) = [rand_i \times v_i^d(t) + \xi(c_i^4 - 0.5)] + a_i^d(t), i = 1, 2, \cdots, d \tag{21}$$

where, c_i^d incorporates the logistic mapping based chaotic behavior which is defined in (22).

$$c_i^d = 4c_{i-1}^d(1 - c_{i-1}^d), i = 1, 2, \cdots, d \tag{22}$$

4.3 *Kbest*-based variants

The methods considered in this category modifies the $Kbest$ function of GSA. As $Kbest$ controls the balance between exploration and exploitation, each method affects the number of considered objects which apply force on others in an iteration to achieve better trade-off.

4.4 Logarithmic Kbest GSA (LKGSA)

LKGSA [31] modifies the $Kbest$ function such that there is logarithmic decrease rather than linearly in the number of objects that are applying force over different iterations. This makes better (or heavier) objects apply force for more iterations. Equation (23) defines the formulation of the logarithmic $Kbest$ at t^{th} iteration, considering P and max_it as the population size and maximum iterations, respectively.

$$Kbest(t) = P \times \frac{final\_per + log\left[1 + \left(\frac{(max\_it)^{final\_per}}{t}\right) \times \left(\frac{P}{t}\right)\right]}{100} \tag{23}$$

In LKGSA, large number of objects are considered for few iterations only which signify that logarithmic $Kbest$ performs exploration at initial stage only. With increasing iterations, logarithmic $Kbest$ considers smaller number of best objects which perform the exploitation of the search space. This makes LKGSA with better convergence rate. However, the exploration ability of LKGSA is poor.

4.5 Chaotic Kbest GSA (CKGSA)

CKGSA [29] modifies the $Kbest$ function with the logistic mapping-based chaotic behavior. Literature has witnessed that chaos has better searching behavior than stochastic search, therefore it helps GSA in escaping the local optima as chaos [9, 13]. Equation (24) defines the formulation of the proposed $Kbest$ at t^{th} iteration.

$$Kbest(t) = P \times \frac{(P - final\_per) \times \left(\frac{max\_it - t}{max\_it}\right) + final\_per \times z(t)}{100} \tag{24}$$

where, $z_{(t)}$ corresponds to the logistic mapping which is defined as (25).

$$z_{(t+1)} = \mu \times z_t \times (1 - z_t), \tag{25}$$

where, z_0 and μ correspond to random value and 'biotic potential' [24]. Above certain value of μ, (25) behaves chaotically [4]. This variant has a demerit of biasness towards initial settings as chaotic behavior is dependent on initial conditions.

4.6 Exponential Kbest GSA (EKGSA)

EKGSA defines the $Kbest$ with an exponential decrease instead of linear decrease [30]. Equation (26) formulates the modified $Kbest$ at t^{th} iteration where max_it and P represent the maximum number of iterations and number of objects, respectively.

$$Kbest(t) = P \times \frac{\left(\frac{final\_per}{P}\right)^{\frac{t}{max\_it}}}{100} \tag{26}$$

In EKGSA, $Kbest$ function starts with exploration and then performs exhaustive exploitation. However, EKGSA still lacks the convergence precision.

5 Experimental results

The variants of the GSA has been experimentally tested against state-of-the-art meta-heuristics. The experiments are performed on 17 standard benchmark functions ($F_1 - F_{17}$) and 28 CEC benchmark functions ($C_1 - C_{28}$) which are produced from IEEE Congress on

Evolutionary Computation (CEC), 2013. The functions include real parameter single objective optimization problems of IEEE Congress on Evolutionary Computation (CEC), 2013, along with the unimodal, and multimodal. Table 1 contains the definitions, range of features, global minimum fitness, optimal position values, and categories of standard benchmark functions ($F_1 - F_{17}$) functions.

Further, the function ($C_1 - C_{28}$) are presented in Table 2 which are real-parameter and single-objective and used to validate the robustness of the algorithm [2]. The performance has been evaluated in terms of mean fitness value and convergence graph. The experiments experiments are performed using a computer with 2.35 GHz with Core i5 processor, 16 GB of RAM and Matlab 2017a.

5.1 Performance analysis

For the performance analysis, nine variants of GSA, namely DGSA [51], OGSA [53], MGSA(I) [18], MGSA(II) [13], AGSA [27], LKGSA, CKGSA, EKGSA, and IGSA has been compared with the standard GSA. Moreover, the results are also compared with seven other nature-inspired algorithms, namely ageist spider monkey optimizer (ASMO) [52], improved salp swarm optimization (ISSA) [14], and modified grasshopper optimization algorithm (MGOA) [25], improved bat algorithm (IBA) [62], modified particle swarm optimization (MPSO) [22], shuffled differential evolutionary (SDE) [36], and spiral biogeography based optimizer (SBBO) [43]. All the considered algorithms are executed over 90, 50, 30, and 10 dimensions on each function. The parameter settings of considered algorithms is taken from the respective literature. The mean and standard deviation of the fitness value was observed by running all the algorithms 30 times on each benchmark function.

The mean fitness values of all the considered algorithms for S_1 set ($F_1 - F_{10}$) and ($F_{11} - F_{17}$) are depicted in Tables 3 and 4. For better comparison, the best three values have been computed and highlighted with red, blue, and green color in the tables where red color represents the first-best value, blue color marks the second-best, and green color depicts the third-best value. It can be observed from the tables that the IGSA returns the first or second-best values over F_1, F_2, F_3, F_{13}, and F_{16} benchmark functions for all the dimensions while CKGSA returns the first or second-best values for F_6 benchmark function. There are two benchmark functions F_9 and F_{10} where other methods perform slightly better than the IGSA. For f_9 benchmark function, ISSA performs the best for all the dimensions except 30 for which EKGSA performs the best. MPSO shows better results for 10, 30, 90 dimensions of F_{10} benchmark function while SDE and GSA perform the best for dimension 10 and 50 respectively. For F_7 and F_8 benchmark functions, ASMO, AGSA, MGOA, and IGSA show better performance whereas SDE, ASMO, OGSA, CKGSA, LKGSA, MGSA, DGSA, and IGSA show better results for benchmark functions F_{11}, F_{12}, F_{14}, F_{15}, F_{17}. From the tables, it is envisioned that the IGSA returns the first or second-best values for more than 88% of benchmark functions over any of the dimensions.

Furthermore, Tables 5, 6, and 7 show results on the S_2 set ($C_1 - C_{10}$), ($C_{11} - C_{20}$), and ($C_{21} - C_{28}$) respectively. The best values returned by considered methods are represented by red color while second and third best values are depicted in blue and green colors respectively. In Tables 5, IGSA show best results on all benchmark problems except C_2, C_4, C_6, and C_9 with 10 dimensions where EKGSA, MPSO, and LKGSA perform better. Moreover, on these problems the results are improved when the problem dimensions are increased. Table 6 shows the performance of considered methods on multimodal functions. Here also, IGSA outperforms on all problems except C_{12} , C_{15} and C_{18} with 10 dimensions where

Table 1 The considered standard benchmark functions [7]

S.No.	Function	Equation	Range	O.V.	O.P.	Category
1.	Ackley	$F_1(X) = -20e^{-0.02\sqrt{d^{-1}\sum_{i=1}^{d} x_i^2}} - e^{d^{-1}\sum_{i=1}^{d} cos(2\pi x_i)} + 20 + e$	[-35 *to* 35]	0	(0,…,0)	MM
2.	Alpine	$F_2(X) = \sum_{i=1}^{d} \lvert x_i \sin(x_i) + 0.1x_i \rvert$	[-10 *to* 10]	0	(0,…,0)	MM
3.	Brown	$F_3(X) = \sum_{i=1}^{d-1} (x_i^2)^{(x_{i+1}^2+1)} + (x_{i+1}^2)^{(x_i^2+1)}$	[-1 *to* 4]	0	(0,…,0)	UM
4.	Dixon and Price	$F_4(X) = (x_1 - 1)^2 + \sum_{i=2}^{d} i(2x_i^2 - x_{i-1})^2$	[-10 *to* 10]	0	$2^{\frac{-(2^i-2)}{(2^i)}}$, i=1,2,…,d	UM
5.	Griewank	$F_5(X) = 1 + \sum_{i=1}^{d} \frac{x_i^2}{4000} - \prod_{i=1}^{d} \cos(\frac{x_i}{\sqrt{i}})$	[-600 *to* 600]	0	(0,…,0)	MM
6.	Pathological	$F_6(X) = \sum_{i=1}^{d-1} \left(0.5 + \frac{\sin^2 \sqrt{100x_i^2 + x_{i+1}^2} - 0.5}{1 + 0.001(x_i^2 - 2x_i x_{i+1} + x_{i+1}^2)^2}\right)$	[-100 *to* 100]	0	(0,…,0)	MM
7.	Quartic	$F_7(X) = \sum_{i=1}^{d} i x_i^4$	[-1.28 *to* 1.28]	0	(0,…,0)	UM
8.	Rosenbrock's	$F_8(X) = \sum_{i=1}^{d-1} [100(x_{i+1} - x_i^2)^2 + (x_i - 1)^2]$	[-30 *to* 30]	0	(1,…,1)	UM
9.	Rosenbrock and Yang's	$F_9(X) = \sum_{i=1}^{d-1} \left(100\epsilon_i (x_{i+1} - x_i^2)^2 + (x_i - 1)^2 \right)$	[-30 *to* 30]	0	(1,…,1)	UM
10.	Rotated Hyper-Ellipsoid	$F_{10}(X) = \sum_{i=1}^{d} \sum_{j=1}^{i} x_j^2$	[-65.536 *to* 65.536]	0	(0,…,0)	UM
11.	Schumer Steiglitz	$F_{11}(X) = \sum_{i=1}^{d} x_i^4$	[-100 *to* 100]	0	(0,…,0)	UM
12.	Schwefel2	$F_{12}(X) = \sum_{i=1}^{d} \left(\sum_{j=1}^{i} x_j \right)^2$	[-65.536 *to* 65.536]	0	(0,…,0)	UM
13.	Schwefel3	$F_{13}(X) = \sum_{i=1}^{d} \lvert x_i \rvert + \prod_{i=1}^{d} \lvert x_i \rvert$	[-10 *to* 10]	0	(0,…,0)	MM
14.	Schwefel4	$F_{14}(X) = \max_i (\lvert x_i \rvert : i\epsilon \{1, \cdots, d\})$	[-100 *to* 100]	0	(0,…,0)	UM
15.	Step	$F_{15}(X) = \sum_{i=1}^{d} (\lfloor \lvert x_i \rvert \rfloor)$	[-100 *to* 100]	0	(0,…,0)	UM
16.	Trigonometric	$F_{16}(X) = \sum_{i=1}^{d} [d - \sum_{j=1}^{d} \cos x_j + i(1 - cos(x_i) - sin(x_i))]^2$	[0 *to* pi]	0	(0,…,0)	MM
17.	Zakharov	$F_{17}(X) = \sum_{i=1}^{d} x_i^2 + (\frac{1}{2} \sum_{i=1}^{d} i x_i)^2 + (\frac{1}{2} \sum_{i=1}^{d} i x_i)^4$	[-5 *to* 10]	0	(0,…,0)	MM

O.V.: Optimal Value; O.P.: Optimal Position; UM : Uni-Modal; MM : Multi-Modal

JrnlID 11042_ArtID 9831_Proof#1 - 13/09/2020

Table 2 Description of considered real-parameter single objective optimization problems of CEC, 2013 [2]

Sr. No.	Function	Range	Optimal value	Category
C_1	Sphere	[-100 *to* 100]	−1400	UM
C_2	Rotated High Conditioned Elliptic	[-100 *to* 100]	−1300	UM
C_3	Rotated Bent Cigar	[-100 *to* 100]	−1200	UM
C_4	Rotated Discus	[-100 *to* 100]	−1100	UM
C_5	Different Powers	[-100 *to* 100]	−1000	UM
C_6	Rotated Rosenbrock	[-100 *to* 100]	−900	MM
C_7	Rotated Schaffers F7	[-100 *to* 100]	−800	MM
C_8	Rotated Ackley	[-100 *to* 100]	−700	MM
C_9	Rotated Weierstrass	[-100 *to* 100]	−600	MM
C_{10}	Rotated Griewank	[-100 *to* 100]	−500	MM
C_{11}	Rastrigin	[-100 *to* 100]	−400	MM
C_{12}	Rotated Rastrigin	[-100 *to* 100]	−300	MM
C_{13}	Non-Continuous Rotated Rastrigin	[-100 *to* 100]	−200	MM
C_{14}	Schwefel	[-100 *to* 100]	−100	MM
C_{15}	Rotated Schwefel	[-100 *to* 100]	100	MM
C_{16}	Rotated Katsuura	[-100 *to* 100]	200	MM
C_{17}	Lunacek Bi_Rastrigin	[-100 *to* 100]	300	MM
C_{18}	Rotated Lunacek Bi_Rastrigin	[-100 *to* 100]	400	MM
C_{19}	Expanded Griewank plus Rosenbrock	[-100 *to* 100]	500	MM
C_{20}	Expanded Scaffer F6	[-100 *to* 100]	600	MM
C_{21}	CP 1 (n=5,Rotated)	[-100 *to* 100]	700	CP
C_{22}	CP 2 (n=3,Unrotated)	[-100 *to* 100]	800	CP
C_{23}	CP 3 (n=3,Rotated)	[-100 *to* 100]	900	CP
C_{24}	CP 4 (n=3,Rotated)	[-100 *to* 100]	1000	CP
C_{25}	CP 5 (n=3,Rotated)	[-100 *to* 100]	1100	CP
C_{26}	CP 6 (n=5,Rotated)	[-100 *to* 100]	1200	CP
C_{27}	CP 7 (n=5,Rotated)	[-100 *to* 100]	1300	CP
C_{28}	CP 8 (n=5,Rotated)	[-100 *to* 100]	1400	CP

UM : Unimodal; MM : Multimodal; CP : Composition

results are improved when dimensions are increased. However, on C_{16} IGSA does not perform well on higher dimensions. For this problem, CKGSA returns good results for higher dimensions. Similarly, Table 7 shows that IGSA performs well on all hybrid and composite problems except C_{23} and C_{28} for 10 and 50 dimensions respectively where OGSA and SBBO outperforms others. From the tables, it can be observed that IGSA shows best mean fitness values on 14, 17, 13, and 17 benchmark functions with 10, 30, 50, and 90 dimensions respectively which is more than 50% in each case. This shows the effectiveness of IGSA as compared to other considered meta-heuristic methods. Moreover, in the remaining cases, it either performs second best or third best. Further, it can be seen that for all benchmark problems, IGSA performs better on one dimension at least while no other algorithm shows better results on 50% of the considered problems. Thus, it can be stated that IGSA attains better trade-off between exploration and exploitation on different complex functions.

Table 3 Comparative analysis of existing and new algorithms for mean fitnes values over 30 runs on the benchmark functions ($F_1 - F_{10}$) for different dimensions

Fn.	D	MPSO	SDE	SBBO	ASMO	ISSA	MGOA	IBA	GSA	DGSA	OGSA	MGSA(I)	MGSA(II)	AGSA	LKGSA	CKGSA	EKGSA	IGSA
F_1	10	2.41E-44	4.78E-28	1.86E-12	8.37E-19	3.65E-18	7.56E-19	8.07E- 04	8.76E+ 01	1.71E-20	1.19E-15	8.78E-23	2.16E+ 00	2.05E-23	7.94E-19	8.29E-19	6.52E-19	5.71E-52
	30	2.47E-14	2.66E-16	2.27E-02	1.40E- 08	6.47E-17	1.09E-17	1.12E-03	4.18E+ 01	2.41E-19	1.20E-14	1.16E+ 02	2.41E+ 01	1.73E-21	1.08E-17	1.06E-17	3.72E- 03	2.91E-27
	50	2.83E- 05	3.45E- 05	1.50E+ 01	1.64E- 04	1.94E+ 03	8.17E-17	8.15E+ 00	4.39E+ 01	2.43E+ 03	8.08E-14	7.41E-106	6.50E+ 01	3.58E-18	1.94E+ 04	2.01E- 16	1.64E-11	1.29E-171
	90	2.50E- 01	5.04E+ 00	1.28E+ 02	1.73E- 04	2.06E+ 04	3.91E- 16	8.94E+ 00	1.39E+ 03	2.69E+ 04	1.77E- 03	4.88E- 104	3.05E+ 02	7.81E+ 00	8.05E+ 04	1.94E- 15	8.31E- 09	1.62E-165
F_2	10	1.06E- 10	3.50E- 15	1.28E+ 02	2.83E- 09	5.85E- 09	2.73E- 09	3.41E- 02	5.48E- 02	3.90E- 10	8.59E- 08	1.60E- 18	4.03E+ 00	1.37E- 11	2.68E- 09	2.61E- 09	2.01E-12	5.98E- 19
	30	3.37E- 21	1.00E- 45	4.16E- 02	3.41E+ 01	2.88E+ 00	1.63E- 08	1.16E- 01	1.59E- 01	2.44E- 09	4.79E- 07	8.81E+ 00	2.97E+ 01	2.05E- 10	1.77E- 08	1.71E- 08	2.70E- 01	9.49E- 221
	50	7.39E- 02	6.45E- 04	1.68E+ 00	2.94E+ 00	5.27E+ 01	6.16E- 08	6.92E+ 00	3.50E-01	1.00E- 01	1.47E- 06	8.73E- 57	5.73E+ 01	2.28E- 04	6.20E-03	8.10E- 08	4.35E- 05	3.44E- 109
	90	3.67E+ 00	8.75E- 01	6.96E+ 00	1.02E+ 01	1.50E+ 02	4.29E- 03	1.14E+ 01	3.36E+ 00	3.01E+ 01	7.33E- 01	2.22E- 55	1.24E+ 02	3.23E- 01	2.67E+ 00	3.51E- 02	1.34E- 02	6.10E- 107
F_3	10	2.53E- 53	3.18E+ 02	1.27E- 04	1.54E- 18	1.23E- 17	1.63E- 18	2.41E- 03	2.48E+ 02	5.57E- 20	2.66E- 15	1.97E- 98	6.64E+ 00	8.66E-23	1.30E- 18	1.46E- 18	5.23E- 69	8.71E- 78
	30	9.70E- 04	7.52E+ 03	1.33E+ 01	3.02E- 03	1.78E+ 03	3.07E- 03	1.62E- 02	9.09E+ 02	9.77E- 18	1.14E- 13	5.61E+ 02	6.06E+ 02	1.59E- 01	1.01E- 16	5.71E-17	2.34E- 02	8.52E- 19
	50	4.13E+ 02	9.68E+ 04	1.30E+ 03	8.86E+ 04	1.54E+ 04	1.63E+ 02	6.36E+ 01	1.18E+ 03	2.67E+ 04	4.05E+ 03	5.09E+03	3.37E+ 03	1.01E+ 03	1.26E+ 05	4.74E+ 02	4.23E+ 02	1.99E- 47
	90	6.00E+ 03	3.37E+ 05	1.56E+ 04	5.79E+ 05	8.64E+ 05	6.92E+ 02	6.11E+ 01	4.18E+ 03	9.04E+ 04	1.45E+ 04	2.83E+04	1.12E+ 04	4.23E+ 03	5.62E+ 05	3.24E+ 03	2.65E+ 03	5.89E- 37
F_4	10	1.18E-61	1.15E-11	2.70E-04	6.43E-10	1.41E-09	6.82E-10	1.73E-02	1.24E-02	1.18E-10	2.35E-08	1.80E-229	8.47E-01	3.79E-12	6.31E-10	6.54E-10	9.72E-06	2.12E-231
	30	9.80E-03	7.78E-07	3.60E-01	1.15E+ 00	2.18E+ 00	2.06E-09	1.56E-02	3.72E-01	4.83E-10	7.56E-08	6.49E+00	2.01E+00	1.26E-10	2.45E-09	2.24E-09	4.02E-02	8.86E-216
	50	2.16E+ 00	2.51E+ 01	2.21E+ 00	4.55E+ 01	1.83E+ 01	3.73E- 05	1.08E+ 00	9.89E+ 00	4.59E+ 01	1.12E- 02	2.26E- 33	7.62E+ 00	4.01E+ 00	3.08E+ 01	1.33E+ 00	1.60E+ 00	8.86E- 216
	90	6.38E+ 00	8.01E+ 01	5.00E+00	6.24E+ 01	2.09E+ 01	1.68E+ 00	9.72E- 01	1.35E+ 01	5.58E+ 01	6.19E+ 00	1.54E+ 01	1.22E+ 01	1.17E+ 01	5.44E+ 01	8.62E+ 00	8.52E+ 00	q2.121E-22

Table 3 (continued)

Fn.	D	MPSO	SDE	SBBO	ASMO	ISSA	MGOA	IBA	GSA	DGSA	OGSA	MGSA(I)	MGSA(II)	AGSA	LKGSA	CKGSA	EKGSA	IGSA
F_5	10	1.69E+ 00	5.86E+ 03	4.30E+ 00	4.84E- 02	2.18E+ 01	4.80E- 02	1.44E- 01	1.97E+ 06	8.95E- 01	6.48E- 03	9.57E+ 00	3.45E+ 02	1.43E- 02	2.73E- 13	4.63E- 05	1.42E+ 00	1.12E- 01
	30	3.67E+ 01	3.02E+ 01	6.50E+ 01	5.70E+ 01	4.43E+ 01	2.24E+ 01	2.66E+ 01	4.10E+ 05	3.22E+ 01	2.19E+ 01	3.27E+ 00	7.71E+ 03	2.16E+ 01	3.10E+ 00	1.87E+ 00	2.26E+ 00	2.00E+ 00
	50	1.34E+ 02	2.02E+ 02	5.54E+ 02	5.18E+ 01	1.21E+ 06	5.09E+ 01	5.31E+ 02	5.19E+ 03	2.85E+ 04	5.74E+ 01	5.38E+ 01	3.23E+ 04	7.07E+ 01	1.22E+ 02	4.92E+ 01	4.86E+ 01	4.02E+ 05
	90	6.84E+ 02	8.88E+ 03	2.30E+ 03	9.61E+ 01	1.84E+ 06	9.51E+ 01	6.02E+ 02	8.35E+ 03	1.85E+ 06	8.08E+ 02	9.77E+ 01	1.45E+ 05	1.16E+03	5.93E+ 04	9.33E+ 01	1.39E+ 02	2.50E+ 06
F_6	10	7.89E-19	7.89E-19	8.60E-19	6.65E-02	4.37E-28	8.30E-04	1.05E-32	1.22E-15	1.99E-23	3.32E-12	4.27E-04	1.03E-32	6.66E- 19	2.24E+ 00	4.22E- 18	1.88E- 20	6.12E- 37
	30	9.78E-18	1.17E-17	1.53E- 08	1.42E+ 02	2.96E- 03	1.23E- 03	2.77E- 32	1.13E-14	2.31E- 21	1.98E-02	2.21E-03	6.34E- 27	1.13E- 17	2.32E+ 01	6.11E-17	2.96E- 19	3.12E- 01
	50	1.13E-16	7.10E-17	4.42E- 02	1.61E+ 00	1.38E-11	6.44E+ 00	1.23E- 04	8.12E- 14	1.74E+02	1.42E+ 01	1.37E+ 01	4.13E- 05	3.86E-18	6.27E+ 01	1.13E+ 03	3.06E+ 03	2.30E+ 02
	90	1.91E- 15	1.63E- 01	5.20E- 01	1.48E+ 01	5.29E- 09	9.83E+ 00	3.98E- 01	8.95E- 04	1.27E+ 01	1.28E+ 02	1.17E+ 03	5.31E+ 00	8.48E+ 04	3.62E+ 02	1.15E+ 04	2.83E+ 04	4.61E-16
F_7	10	6.55E- 03	1.42E-03	2.94E-03	5.01E- 06	1.27E- 02	3.87E- 05	4.90E-04	4.66E-03	6.76E-04	1.70E- 04	2.63E+ 01	1.18E- 03	9.81E- 03	4.14E- 01	7.87E- 03	7.42E- 04	4.92E- 04
	30	4.79E-02	9.81E-03	7.62E- 03	8.59E+ 00	1.20E-01	6.01E- 05	9.63E-03	2.38E- 02	3.70E- 03	8.66E- 04	1.18E+02	5.06E- 03	8.76E- 02	3.25E+ 01	9.30E- 02	7.59E- 03	7.32E- 06
	50	1.40E- 01	2.52E- 02	1.52E- 03	8.78E- 02	1.26E- 01	8.12E- 03	3.30E- 01	8.68E-02	4.51E-02	1.02E-02	1.08E+ 02	8.59E- 02	4.04E-01	1.89E+02	6.08E+ 00	1.33E- 01	3.39E- 05
	90	3.71E- 01	8.12E- 02	8.39E- 04	5.24E- 01	4.10E- 01	1.70E- 02	7.13E+02	5.20E- 01	3.94E- 01	3.71E- 02	1.49E+ 02	4.25E- 01	3.59E- 05	8.31E+ 02	5.21E+ 01	9.40E- 01	1.82E+ 02
F_8	10	5.76E+ 02	6.26E+ 02	6.33E+ 02	5.31E+ 02	5.78E+ 02	2.29E+ 03	5.62E+ 02	4.81E+ 02	4.31E+ 02	1.59E+ 03	5.55E+ 02	1.30E+ 03	5.63E+ 02	4.62E+ 02	1.11E+ 03	9.44E+ 02	2.10E+ 03
	30	5.80E+ 02	6.94E+ 02	3.79E+ 03	1.49E+ 03	5.99E+ 02	1.15E+ 04	5.29E+ 03	1.76E+ 03	2.50E+ 03	6.95E+ 03	6.80E+ 02	1.13E+ 04	8.31E+ 02	4.80E+ 03	7.60E+ 02	5.56E+ 03	3.92E+ 02
	50	1.17E+ 03	1.70E+ 03	1.94E+ 03	1.64E+ 03	1.31E+ 03	6.70E+ 02	1.77E+ 03	1.64E+ 03	2.06E+ 03	1.99E+ 03	1.80E+ 04	8.93E+ 03	9.93E+ 03	8.27E+ 03	1.23E+ 04	1.21E+ 04	1.98E+ 04
	90	2.30E+ 03	3.01E+ 03	2.73E+ 03	2.61E+ 03	2.70E+ 03	1.38E+ 03	3.04E+ 03	2.92E+ 03	4.08E+ 03	3.64E+ 03	3.74E+ 04	1.78E+ 04	1.72E+ 04	1.23E+ 04	2.19E+ 04	1.64E+ 04	3.45E+ 04

First Best value; Second Best value; Third Best value

Table 4 Comparative analysis of existing and new algorithms for mean fitness values over 30 runs on the benchmark functions ($F_{11} - F_{17}$) for different dimensions

Fn.	D	MPSO	SDE	SBBO	ASMO	ISSA	MGOA	IBA	GSA	DGSA	OGSA	MGSA(I)	MGSA(II)	AGSA	LKGSA	CKGSA	EKGSA	IGSA
F_9	10	1.02E+ 00	5.99E+ 00	1.29E+ 01	1.26E+ 20	6.22E- 01	2.22E+ 01	1.34E+ 01	6.50E+ 01	3.97E+ 00	2.81E+ 00	3.26E+ 00	4.00E+ 01	1.55E+ 00	6.27E+ 00	8.71E+ 00	2.08E+ 01	3.43E+ 00
	30	1.01E+ 00	2.41E+ 01	1.25E+ 01	6.05E+ 12	1.39E+ 00	1.13E+ 02	5.66E+ 04	1.93E+ 02	2.17E+ 01	1.53E+ 01	7.33E+ 01	2.44E+ 02	3.12E+ 01	3.49E+ 01	3.60E+ 01	3.66E- 10	1.18E+ 01
	50	1.32E+ 01	6.36E+ 01	5.08E+ 01	7.68E+ 08	9.95E- 01	1.93E+ 02	1.19E+ 02	3.46E+ 02	4.16E+ 01	3.31E+ 01	2.59E+ 01	4.93E+ 02	1.22E+ 02	7.58E+ 01	7.80E+ 01	2.16E+ 02	1.07E+ 02
	90	5.73E+ 02	1.46E+ 02	9.18E+ 01	2.88E+ 07	3.38E+ 00	4.88E+ 02	1.72E+ 02	1.07E+ 02	8.47E+ 01	7.39E+ 01	1.34E+ 01	9.81E+ 02	3.73E+ 02	1.86E+ 02	2.03E+ 02	6.34E+ 02	3.81E+ 02
F_{10}	10	3.26E-15	1.28E-09	4.81E-15	1.56E+ 00	1.38E-09	6.47E-03	1.31E-09	9.77E-16	4.68E-08	6.53E-12	1.38E-09	3.44E+ 00	4.81E-15	2.10E-10	4.18E-07	4.26E-02	3.12E-02
	30	9.10E-16	2.70E-09	5.17E-02	3.33E-01	2.53E-09	1.53E-01	2.56E-09	6.37E+00	8.50E-08	3.69E-11	2.24E+00	5.26E+00	1.31E-14	4.80E-10	3.79E-02	8.63E-15	2.58E-02
	50	7.42E+ 00	9.77E- 16	1.67E- 06	5.65E- 01	5.60E- 09	1.13E+ 01	6.47E+ 00	5.57E+ 00	1.63E- 07	1.27E- 09	5.24E-15	6.13E+ 00	2.47E- 01	1.07E+ 01	1.34E+ 00	1.45E- 03	3.04E+ 00
	90	9.12E-16	2.12E- 08	3.44E- 01	1.35E+ 00	8.98E- 09	1.10E+ 01	8.86E+ 00	3.44E+ 00	8.00E-01	4.26E-01	4.53E- 15	6.75E+ 00	2.00E+ 00	1.76E+ 01	3.03E+ 00	7.78E- 01	3.19E+ 00
F_{11}	10	1.11E- 01	1.71E- 01	3.00E- 02	3.35E- 03	4.65E- 02	3.67E- 03	7.00E- 04	5.32E+ 10	2.84E- 01	4.19E- 03	9.14E- 04	2.65E- 01	3.88E- 03	1.18E+ 00	5.10E- 03	8.47E- 03	2.08E- 05
	30	1.65E- 02	1.03E- 01	6.93E- 02	1.38E- 02	2.10E+ 02	6.17E+ 02	7.07E- 04	2.62E+ 59	1.13E+ 00	1.55E-16	1.17E+ 00	7.91E- 01	1.97E- 03	1.88E+ 01	2.65E+ 01	8.48E- 04	1.40E- 05
	50	8.13E- 03	1.88E- 04	1.23E+ 00	5.23E+ 01	1.31E+ 03	1.78E+ 01	9.51E- 01	1.58E+ 118	8.57E+ 01	5.66E- 03	1.99E+ 00	1.93E+ 01	1.75E+ 01	1.01E+ 03	4.82E+ 01	1.69E+ 01	2.90E+ 00
	90	1.56E-02	1.10E+ 00	2.24E+ 00	1.42E- 02	2.45E+ 03	5.53E+ 01	8.05E- 01	1.47E+ 125	4.85E+ 02	6.33E- 02	1.53E- 02	4.83E+ 01	4.96E+ 01	2.06E+ 03	3.06E+ 02	5.83E+ 01	2.90E+ 00
F_{12}	10	1.39E- 24	8.05E- 02	1.76E- 14	1.70E- 20	7.21E- 02	1.74E- 01	2.27E- 05	2.72E+ 11	3.44E- 22	2.84E-17	7.70E- 03	1.39E- 01	3.82E- 25	7.90E- 01	1.34E- 20	4.61E- 06	4.71E- 32
	30	1.86E- 32	1.58E- 32	4.88E- 05	6.65E+ 00	5.23E+ 00	4.15E- 02	9.40E- 06	9.72E+ 07	5.18E- 02	8.65E- 17	5.38E+ 00	6.77E- 01	1.29E- 23	3.65E- 01	6.20E- 20	1.04E- 02	9.34E- 03
	50	1.36E- 32	2.29E- 05	2.45E- 02	3.78E-03	4.91E+02	1.24E- 02	2.59E- 02	1.28E+ 01	1.51E+ 01	2.49E- 02	8.62E- 01	6.49E+ 00	1.74E- 01	9.44E+ 00	4.98E- 02	5.60E- 02	8.39E+ 00
	90	4.62E- 01	1.33E+ 01	2.33E- 01	1.19E+ 01	7.22E+ 03	2.43E- 02	1.36E- 02	4.62E+ 02	6.03E+ 06	1.87E+ 00	1.16E+ 00	1.99E+ 01	2.04E+ 00	1.71E+ 04	7.56E- 01	7.68E- 01	5.98E- 03
F_{13}	10	1.35E- 32	3.56E- 03	1.42E- 13	7.59E- 20	1.22E- 03	8.90E-20	1.00E- 04	1.49E+ 291	1.75E- 21	1.32E- 16	2.67E- 02	3.73E- 01	7.44E- 24	7.79E-20	1.70E-04	2.61E-04	1.76E-24
	30	2.20E- 03	8.27E- 02	6.37E- 04	5.40E- 03	6.79E- 01	1.01E- 18	1.49E- 04	1.64E+ 208	2.81E- 20	1.23E- 15	3.84E+ 03	7.64E+ 00	1.72E- 22	3.45E- 01	1.10E- 03	2.52E-03	1.35E-32
	50	3.32E- 03	1.08E- 04	6.12E- 01	2.44E-01	6.33E+ 04	2.15E+01	6.26E- 01	4.06E+ 53	4.36E+ 02	1.14E- 01	3.47E+ 00	4.41E+ 01	1.92E+ 00	1.04E+ 02	2.20E- 03	1.24E- 01	5.84E-18
	90	1.11E+ 00	1.22E+ 02	5.23E+ 00	8.14E- 01	2.11E+ 06	1.89E+ 02	6.83E- 01	4.89E+ 47	3.09E+ 07	4.58E+ 01	9.88E+ 00	8.91E+ 02	6.32E+ 01	1.54E+ 06	1.67E+ 00	1.01E- 03	2.33E- 01

Table 4 (continued)

Fn.	D	MPSO	SDE	SBBO	ASMO	ISSA	MGOA	IBA	GSA	DGSA	OGSA	MGSA(I)	MGSA(II)	AGSA	LKGSA	CKGSA	EKGSA	IGSA
F_{14}	10	1.28E+ 00	2.58E-01	3.39E+ 00	5.95E- 01	7.11E-01	4.33E+ 00	3.91E- 01	4.27E+ 02	2.20E- 03	3.34E- 02	5.03E- 01	2.15E- 03	5.36E- 01	1.87E- 03	5.57E- 01	6.97E- 01	2.14E- 02
	30	1.48E+ 00	2.20E- 03	3.54E+ 00	2.20E- 03	4.96E- 01	5.12E+ 00	2.09E- 01	3.37E+ 02	2.20E- 03	6.51E- 03	2.15E+ 00	1.86E- 03	4.97E- 01	5.35E+ 00	2.25E-01	1.05E+ 00	4.53E- 01
	50	8.89E-01	2.20E- 03	3.35E+ 00	2.35E+ 00	2.56E+ 00	2.38E+ 00	2.11E+ 00	1.57E+ 02	3.98E- 01	6.00E- 01	2.38E+ 00	4.42E- 02	1.98E+ 00	5.26E+ 00	2.20E- 03	3.76E+ 00	3.48E+ 00
	90	5.96E- 01	2.00E- 03	4.20E+ 00	5.96E- 01	3.30E+ 00	2.78E+ 00	2.51E+ 00	1.54E+ 02	3.32E+ 00	7.49E- 01	1.24E+00	2.17E- 02	1.29E+ 00	4.39E+ 00	2.77E+ 00	4.05E+ 00	2.00E- 03
F_{15}	10	2.43E-04	1.12E-03	1.03E-03	1.00E-03	1.60E-03	1.12E-04	1.54E-03	3.16E+ 04	3.01E-05	6.82E-04	3.62E-04	7.69E-04	3.63E-04	3.18E-04	5.48E-04	7.86E-06	2.72E-05
	30	4.22E-04	1.12E-04	2.28E-03	2.39E-03	9.72E-04	1.86E-04	1.29E-03	3.70E+ 04	7.56E-06	6.22E-04	1.81E-03	8.61E-04	3.58E-04	1.11E-03	4.79E-04	2.16E-04	3.12E-04
	50	4.74E-04	3.33E-04	2.60E-03	4.36E-04	4.41E-03	3.13E-04	3.65E-03	9.63E+ 02	1.57E-04	1.60E-03	9.09E-04	1.26E-03	8.92E-04	1.48E-03	9.37E-04	4.98E-04	7.49E-06
	90	5.53E-04	4.37E-04	3.47E-04	3.30E-04	3.61E-03	2.19E-04	4.57E-03	9.60E+ 02	2.74E-04	1.75E-03	6.43E-04	1.54E- 03	7.87E-04	1.90E-03	8.92E-04	2.90E-03	7.49E-06
F_{16}	10	3.13E-05	3.13E-05	3.13E-05	3.13E-05	4.13E-05	3.13E-05	3.12E-05	5.90 E+04	3.13E-05	3.13E-05	2.92E-04	1.81E-04	3.13E-05	3.13E-05	2.59E-05	3.06E-05	2.85E-05
	30	3.13E-05	3.13E-05	3.13E-05	3.13E-05	3.13E-05	3.13E-05	3.12E-05	2.50E+ 04	3.13E-05	3.13E-05	2.91E-05	1.22E-04	3.13E-05	3.13E-05	3.13E-05	3.05E-05	2.59E-05
	50	3.13E-05	3.13E-05	3.13E-05	3.13E-05	2.18E-04	3.13E-05	3.09E-05	3.52E+ 03	3.13E-05	3.13E-05	1.01E-03	8.51E-04	3.13E-05	3.13E-05	3.13E-05	3.13E-05	1.70E-05
	90	3.13E-05	3.13E-05	3.13E-05	3.13E-05	2.36E-04	3.13E-05	3.11E-05	1.32E+ 03	3.13E-05	3.13E-05	1.47E-03	7.93E-04	3.13E-05	3.13E-05	3.13E-05	3.13E-05	1.87E-05
F_{17}	10	8.28E-14	8.55E-14	5.82E-01	8.17E-14	8.36E-14	3.01E+ 00	1.52E-07	4.95E+ 06	8.42E-14	6.44E-14	2.03E-02	5.99E-03	8.42E-14	8.22E-14	8.53E-14	4.42E-05	3.92E-14
	30	8.61E-14	8.65E-14	2.70E+ 00	2.95E-14	7.51E-14	1.02E+ 00	1.52E-07	2.70E+ 06	8.62E-14	6.55E-14	2.09E-02	5.48E-03	8.57E-14	8.50E-14	8.57E-14	4.96E-05	2.51E-02
	50	7.00E-14	8.65E-14	7.66E-14	1.41E-06	7.33E-14	1.51E+ 00	8.47E-07	5.81E+ 05	8.28E-14	4.85E-14	8.38E-02	3.01E-02	8.42E-14	8.23E-14	8.23E-14	6.66E-14	4.17E-14
	90	8.60E-14	8.65E-14	7.04E-14	1.69E-06	8.06E-14	1.87E+ 00	1.00E-06	7.01E+ 04	8.41E-14	2.06E-06	8.89E-02	3.68E-02	8.46E-14	7.53E-14	4.42E-14	6.11E-14	5.44E-02

First Best value; Second Best value; Third Best value

Table 5 Comparative analysis of existing and new algorithms for mean fitness values over 30 runs on the CEC2013 benchmark functions ($C_1 - C_{10}$) for considered dimensions

Fn.	D	MPSO	SDE	SBBO	ASMO	ISSA	MGOA	IBA	GSA	DGSA	OGSA	MGSA(I)	MGSA(II)	AGSA	LKGSA	CKGSA	EKGSA	IGSA
C_1	10	4.41E-14	1.64E-06	2.53E-10	2.14E+00	1.55E+01	6.19E-10	3.26E-11	3.15E-04	3.67E-10	1.76E-09	4.34E-01	2.45E+00	5.17E-10	2.12E-09	8.10E-10	1.62E-10	3.74E-12
	30	5.46E-13	2.27E-13	7.28E-02	1.59E-13	2.50E-13	1.36E-13	5.59E+04	3.79E+03	2.05E-13	3.97E+04	1.30E+00	2.52E+01	2.27E-13	3.44E+03	2.50E-13	4.32E-13	1.17E-13
	50	2.14E+00	3.53E-05	1.52E+01	1.24E+04	7.77E+04	3.06E+04	9.01E+04	4.71E+04	1.06E+04	6.10E+03	1.47E+04	1.10E+04	1.15E+04	8.13E+04	1.49E+03	6.41E-13	6.62E-13
	90	4.54E+02	3.44E+00	1.27E+02	8.30E+04	2.18E+05	1.07E+05	1.83E+05	1.38E+05	7.48E+04	4.60E+01	7.26E+04	8.07E+04	7.65E+04	2.04E+05	5.28E+04	6.82E+04	1.20E-12
C_2	10	3.47E+05	2.34E+04	1.33E+05	1.09E+06	5.47E+06	9.30E+05	3.47E+06	1.04E+06	8.56E+04	2.08E+05	6.08E+06	4.13E+06	9.15E+05	4.39E+05	9.80E+03	4.94E+03	1.67E+06
	30	1.67E+07	8.36E+07	3.96E+06	6.98E+06	3.03E+07	5.21E+06	1.83E+09	3.96E+07	2.18E+08	6.21E+08	2.64E+07	2.12E+07	6.26E+06	7.83E+07	7.58E+05	2.95E+06	1.21E+02
	50	9.40E+07	6.19E+08	1.69E+07	1.14E+08	3.71E+09	3.23E+08	4.02E+09	1.19E+09	5.97E+08	2.50E+07	1.93E+08	1.55E+08	1.07E+08	3.16E+09	7.34E+07	7.01E+07	2.01E+06
	90	4.45E+07	6.38E+08	1.43E+07	1.41E+09	1.48E+10	2.32E+09	9.69E+09	4.39E+09	1.87E+09	4.39E+07	2.05E+09	1.67E+09	1.18E+09	9.43E+09	7.68E+08	1.04E+09	4.54E+05
C_3	10	2.70E+05	4.11E+07	2.44E+07	5.32E+07	1.99E+09	2.98E+08	4.67E+07	4.53E+08	7.36E+06	2.46E+05	2.84E+08	3.27E+08	7.09E+07	5.77E+07	3.28E+06	3.30E+04	1.66E+00
	30	3.01E+08	1.88E+08	3.02E+08	5.87E+09	4.11E+10	3.78E+09	1.26E+20	7.78E+10	1.95E+12	1.41E+16	1.82E+10	8.15E+09	4.05E+09	1.85E+14	3.64E+08	7.25E+06	1.60E+07
	50	1.78E+10	5.35E+10	1.20E+09	1.65E+11	1.76E+23	3.42E+11	1.14E+17	1.29E+14	5.34E+11	8.14E+09	8.39E+11	4.23E+11	1.02E+11	1.34E+17	3.50E+10	5.71E+10	1.17E+08
	90	4.24E+10	5.34E+10	4.19E+09	8.60E+17	3.50E+28	2.19E+17	5.67E+21	5.79E+19	5.69E+18	2.44E+12	3.31E+18	1.11E+18	1.53E+18	3.70E+24	6.71E+13	5.23E+15	2.43E+08
C_4	10	5.59E+02	1.50E+04	1.93E+03	1.83E+04	1.97E+04	1.94E+04	9.38E+03	1.99E+04	4.97E+01	1.38E+04	1.82E+04	1.12E+04	1.81E+04	1.36E+04	2.01E+04	4.90E-13	8.55E+03
	30	8.35E+03	6.97E+04	1.20E+03	7.98E+04	7.59E+04	7.42E+04	7.49E+04	7.75E+04	3.04E+04	6.90E+04	7.38E+04	7.14E+04	7.37E+04	6.53E+04	7.30E+04	7.30E+04	2.04E-08
	50	7.81E+04	1.92E+05	6.11E+04	1.04E+05	4.68E+07	9.83E+04	1.44E+05	1.06E+05	1.45E+05	1.07E+05	1.04E+05	9.80E+04	1.04E+05	3.50E+05	1.08E+05	1.03E+05	3.32E+02
	90	1.57E+05	2.38E+05	4.18E+04	1.95E+05	1.38E+09	1.90E+05	2.84E+05	1.91E+05	2.63E+05	2.02E+05	2.00E+05	1.97E+05	1.88E+05	6.61E+06	1.82E+05	1.81E+05	4.79E+02
C_5	10	1.03E-13	4.05E-04	3.77E-06	2.83E-05	6.38E-04	2.94E-05	3.66E-08	4.14E-02	7.78E-04	1.94E-10	2.21E+01	1.33E+01	2.84E-09	2.45E-15	1.79E-12	1.13E-13	2.12E-15
	30	2.73E-11	1.14E-13	1.43E-01	3.33E-10	2.63E+02	2.44E-10	3.66E+04	9.22E+02	1.73E-12	1.55E+04	6.73E+01	7.90E+01	5.66E-12	5.07E+02	1.02E-12	4.09E-13	8.17E-13
	50	6.76E+00	5.29E-03	5.48E+00	1.78E+03	1.80E+04	2.86E+03	2.81E+04	6.28E+03	1.67E+03	1.62E+02	2.63E+03	1.88E+03	1.62E+03	2.71E+04	3.64E+02	8.79E+02	7.85E-09
	90	2.57E+02	9.65E+00	4.10E+01	1.65E+04	1.01E+05	1.97E+04	9.56E+04	3.70E+04	1.51E+04	1.04E+03	2.32E+04	1.69E+04	1.56E+04	1.36E+05	5.07E+03	1.01E+04	3.62E-08
C_6	10	6.18E+00	1.07E+01	7.69E+00	4.79E+01	4.12E+01	4.07E+01	1.22E+01	2.86E+01	8.13E+00	1.04E+01	7.37E+01	5.31E+01	4.88E+01	2.34E+01	1.22E+01	8.26E+00	9.81E+00
	30	8.70E+01	2.71E+01	5.73E+01	8.63E+01	1.24E+02	5.63E+01	1.68E+04	4.27E+02	1.59E+03	7.32E+03	1.03E+02	7.96E+01	7.59E+01	1.38E+03	7.03E+01	1.02E+01	5.01E+01
	50	7.91E+01	5.27E+01	6.94E+01	7.27E+02	1.04E+04	1.98E+03	1.31E+04	4.19E+03	2.18E+03	9.29E+01	9.10E+02	7.76E+02	6.10E+02	1.04E+04	3.25E+02	4.03E+02	4.45E+01
	90	7.20E+02	4.89E+02	3.33E+02	1.41E+04	4.83E+04	1.99E+04	4.93E+04	2.90E+04	2.15E+04	8.50E+02	1.52E+04	1.46E+04	1.28E+04	6.10E+04	9.87E+03	1.09E+04	2.07E+02

Table 5 (continued)

Fn.	D	MPSO	SDE	SBBO	ASMO	ISSA	MGOA	IBA	GSA	DGSA	OGSA	MGSA(I)	MGSA(II)	AGSA	LKGSA	CKGSA	EKGSA	IGSA
C_7	10	3.69E+00	4.52E+04	5.91E+01	1.37E+01	7.71E+01	3.17E+01	1.68E+01	7.07E+01	2.12E+01	6.12E+00	2.13E+01	2.53E+01	1.23E+01	1.22E+02	6.92E+00	3.56E-01	5.32E-06
	30	4.46E+01	7.73E+01	1.24E+02	7.15E+01	1.51E+04	8.52E+01	1.74E+07	1.83E+06	1.12E+03	7.16E+04	8.26E+01	9.30E+01	6.86E+01	1.51E+05	7.12E+01	2.47E+01	1.98E+01
	50	1.51E+02	2.02E+02	1.39E+02	7.91E+02	3.41E+09	7.00E+03	3.17E+05	1.36E+05	7.67E+02	7.23E+01	1.16E+03	3.22E+02	2.12E+03	1.21E+05	3.00E+02	3.89E+02	5.54E+01
	90	1.45E+02	1.74E+02	1.33E+02	6.74E+05	4.24E+10	2.11E+06	8.20E+06	8.90E+06	2.80E+05	5.11E+02	8.89E+05	1.84E+05	1.14E+06	3.55E+07	2.93E+05	5.94E+05	9.42E+01
C_8	10	2.78E+01	2.57E+01	2.89E+01	2.68E+01	2.35E+01	3.89E+01	2.79E+01	3.66E+01	4.88E+01	3.45E+01	4.00E+01	3.01E+01	3.44E+01	2.35E+01	2.79E+01	2.46E+01	2.02E+01
	30	2.64E+01	4.62E+01	3.96E+01	3.74E+01	5.17E+01	3.63E+01	3.41E+01	3.85E+01	2.41E+01	2.52E+01	2.53E+01	2.64E+01	2.52E+01	2.64E+01	2.53E+01	2.86E+01	2.08E+01
	50	2.55E+01	3.54E+01	3.76E+01	3.87E+01	2.45E+01	2.55E+01	3.76E+01	3.65E+01	2.66E+01	2.44E+01	3.65E+01	2.77E+01	2.44E+01	3.32E+01	2.55E+01	2.66E+01	2.11E+01
	90	2.90E+01	3.44E+01	3.33E+01	2.49E+01	2.87E+01	2.17E+01	2.35E+01	2.33E+01	3.41E+01	3.28E+01	3.45E+01	3.12E+01	3.82E+01	2.57E+01	2.61E+01	2.74E+01	2.23E+01
C_9	10	3.29E+00	1.11E+01	6.65E+00	3.73E+00	6.01E+00	1.02E+01	4.35E+00	5.33E+00	4.83E+00	1.40E+00	4.57E+00	5.22E+00	3.40E+00	1.23E+00	4.97E+00	2.47E+00	5.33E+00
	30	2.56E+01	4.03E+01	2.97E+01	3.50E+01	3.69E+01	4.28E+01	5.00E+01	5.01E+01	3.73E+01	4.75E+01	3.82E+01	3.88E+01	3.38E+01	4.04E+01	3.35E+01	1.95E+01	7.03E+00
	50	5.90E+01	8.20E+01	5.94E+01	6.46E+01	8.12E+01	7.71E+01	8.85E+01	8.43E+01	7.44E+01	2.68E+01	6.81E+01	7.22E+01	6.74E+01	8.39E+01	6.73E+01	6.40E+01	3.47E+01
	90	9.39E+01	1.46E+02	8.72E+01	1.43E+02	1.67E+02	1.52E+02	1.74E+02	1.68E+02	1.39E+02	5.46E+01	1.50E+02	1.52E+02	1.42E+02	1.73E+02	1.40E+02	1.40E+02	5.29E+01
C_{10}	10	5.35E-01	8.55E-02	1.57E+00	4.20E-03	9.30E-02	2.39E-03	2.51E+00	5.42E-01	3.85E-01	2.23E-03	1.25E+00	1.50E+00	5.32E-03	7.41E-02	1.81E-03	7.05E-02	7.62E-04
	30	8.77E-01	3.90E+01	2.22E+00	1.02E-01	6.01E+01	2.34E-02	9.94E+03	9.30E+02	1.76E+03	6.06E+03	6.78E+00	6.62E+00	1.23E-01	1.60E+03	4.83E-03	5.08E-02	1.26E-02
	50	1.70E+02	1.76E+03	1.99E+01	1.70E+03	1.26E+04	3.78E+03	1.59E+04	6.88E+03	5.58E+03	3.76E+01	2.12E+03	1.65E+03	1.47E+03	1.32E+04	8.00E+02	1.17E+03	2.22E-01
	90	3.17E+02	1.40E+03	5.00E+01	1.06E+04	3.60E+04	1.57E+04	3.41E+04	2.26E+04	1.63E+04	4.82E+02	1.24E+04	1.09E+04	1.09E+04	3.46E+04	5.71E+03	8.51E+03	8.64E-02

First Best value; Second Best value; Third Best value

Table 6 Comparative analysis of existing and new algorithms for mean fitness values over 30 runs on the CEC2013 benchmark functions ($C_{11} - C_{20}$) for considered dimensions

Fn.	D	MPSO	SDE	SBBO	ASMO	ISSA	MGOA	IBA	GSA	DGSA	OGSA	MGSA(I)	MGSA(II)	AGSA	LKGSA	CKGSA	EKGSA	IGSA
C_{11}	10	1.80E+00	2.47E+02	2.56E+00	1.96E+01	3.40E+01	1.86E+02	5.85E-04	1.44E+02	2.25E+01	3.88E+00	2.02E+01	2.63E+01	1.99E+01	5.98E+01	2.92E+01	6.67E+00	1.95E-07
	30	2.87E+01	1.99E+01	2.64E+01	3.02E+02	4.54E+02	7.48E+02	9.55E+02	7.64E+02	2.42E+02	7.74E+02	3.17E+02	4.19E+02	3.21E+02	5.10E+02	3.60E+02	5.32E+01	2.86E+01
	50	1.33E+02	2.19E+02	1.39E+02	7.18E+02	1.27E+03	9.65E+02	1.32E+03	8.91E+02	6.93E+02	1.44E+02	6.92E+02	8.98E+02	7.43E+02	1.34E+03	6.65E+02	6.92E+02	9.89E+01
	90	4.37E+02	6.34E+02	4.98E+02	1.96E+03	3.27E+03	2.33E+03	3.14E+03	2.38E+03	1.93E+03	4.67E+02	2.02E+03	2.36E+03	1.96E+03	3.79E+03	1.80E+03	1.70E+02	3.20E+02
C_{12}	10	1.48E+01	2.61E+02	2.15E+01	1.55E+01	3.46E+01	1.60E+02	1.07E+01	1.54E+02	2.00E+01	3.41E+00	1.64E+01	1.82E+01	1.56E+01	5.41E+01	2.63E+00	1.05E+01	1.33E+01
	30	1.10E+02	2.15E+02	1.18E+02	3.69E+02	5.01E+02	8.97E+02	9.71E+02	8.35E+02	3.84E+02	7.51E+02	3.62E+02	4.05E+02	3.74E+02	4.78E+02	4.69E+01	6.06E+01	1.61E+01
	50	4.44E+02	5.34E+02	2.39E+02	1.01E+03	1.73E+03	1.12E+03	1.46E+03	1.08E+03	8.94E+02	9.17E+02	1.02E+03	1.09E+03	9.98E+02	6.94E+01	4.43E+02	9.59E+02	1.35E+02
	90	7.91E+02	1.11E+03	6.97E+02	2.25E+03	3.60E+03	2.57E+03	3.40E+03	2.49E+03	2.30E+03	1.04E+03	2.35E+03	2.53E+03	2.25E+03	3.67E+02	1.37E+03	2.22E+03	3.86E+02
C_{13}	10	2.05E+01	2.86E+02	3.82E+01	3.57E+01	6.15E+01	1.77E+02	2.05E+01	1.72E+02	3.44E+01	6.39E+00	3.72E+01	3.46E+01	3.19E+01	4.32E+00	9.12E+01	1.80E+01	1.44E+01
	30	1.93E+02	2.20E+02	1.94E+02	4.97E+02	7.56E+02	9.81E+02	9.97E+02	9.69E+02	5.65E+02	7.32E+02	4.97E+02	4.51E+02	5.05E+02	6.47E+02	1.10E+02	1.26E+02	4.27E+01
	50	5.30E+02	5.23E+02	3.47E+02	1.20E+03	1.92E+03	1.42E+03	1.48E+03	1.37E+03	9.47E+02	1.94E+02	1.14E+03	1.10E+03	1.23E+03	1.35E+03	5.70E+02	1.24E+03	2.36E+02
	90	9.54E+02	1.09E+03	7.33E+02	2.62E+03	4.11E+03	3.01E+03	3.33E+03	3.02E+03	2.44E+03	1.05E+03	2.70E+03	2.60E+03	2.64E+03	3.93E+03	1.80E+03	2.65E+03	5.76E+02
C_{14}	10	1.02E+02	1.66E+03	3.37E+02	7.87E+02	1.38E+03	1.80E+03	1.88E-01	1.51E+03	8.72E+02	3.99E+02	8.32E+02	8.86E+02	7.61E+02	1.32E+03	4.69E+02	2.04E+02	1.03E-01
	30	8.88E+02	7.54E+02	1.32E+03	3.93E+03	5.40E+03	5.72E+03	7.61E+03	5.91E+03	3.41E+03	8.73E+03	3.90E+03	5.15E+03	3.93E+03	5.37E+03	3.15E+03	2.20E+03	2.08E+03
	50	4.12E+03	6.28E+03	3.86E+03	8.03E+03	1.07E+04	9.38E+03	1.62E+04	9.37E+03	7.29E+03	5.54E+03	8.80E+03	1.08E+04	8.25E+03	1.71E+04	6.95E+03	7.16E+02	3.38E+03
	90	1.20E+04	2.04E+04	1.20E+04	1.60E+04	2.35E+04	1.76E+04	3.12E+04	1.85E+04	1.82E+04	1.20E+04	1.74E+04	2.26E+04	1.65E+04	3.31E+04	1.39E+04	1.51E+04	4.32E+03
C_{15}	10	8.63E+02	1.43E+03	1.12E+03	4.83E+02	1.14E+03	1.17E+03	1.58E+03	1.06E+03	8.29E+02	2.26E+02	4.15E+02	5.02E+02	4.38E+02	9.30E+02	1.99E+02	6.95E+02	1.04E+03
	30	7.57E+03	8.26E+03	4.53E+03	3.76E+03	4.76E+03	4.81E+03	6.04E+03	5.33E+03	4.80E+03	8.26E+03	4.11E+03	4.94E+03	4.29E+03	4.64E+03	2.74E+03	3.35E+03	1.21E+03
	50	1.59E+04	1.64E+04	9.25E+03	9.92E+03	1.15E+04	1.05E+04	1.71E+04	1.10E+04	1.09E+04	1.64E+04	9.89E+03	1.27E+04	1.05E+04	1.77E+04	5.65E+03	9.85E+03	6.71E+03
	90	2.23E+04	2.81E+04	1.50E+04	1.58E+04	2.25E+04	1.60E+04	3.23E+04	1.83E+04	1.96E+04	3.18E+04	1.71E+04	2.26E+04	1.56E+04	3.30E+04	1.52E+04	9.75E+03	1.03E+04
C_{16}	10	9.71E-01	7.04E-03	4.40E-01	6.70E-03	1.86E-01	7.56E-03	1.42E+00	2.24E-01	3.14E-01	4.56E-03	1.08E+00	1.20E+00	1.03E-02	4.12E-02	5.04E-03	7.44E-01	2.38E-03
	30	2.77E+00	2.73E+00	1.70E+00	7.79E-03	3.12E-01	7.45E-03	3.36E+00	3.10E-01	3.48E-01	2.94E+00	1.37E+00	2.99E+00	1.03E-02	4.62E-02	6.40E-03	2.21E+00	5.49E-03
	50	4.31E+00	4.32E+00	3.76E+00	5.07E-02	1.75E+00	3.82E-02	4.95E+00	5.43E-01	1.40E+00	3.63E-02	1.56E+00	4.46E+00	5.68E-02	5.14E+00	2.68E-02	3.28E-02	3.10E+00
	90	4.49E+00	4.64E+00	2.53E+00	3.62E-02	2.08E+00	2.01E-02	5.53E+00	2.92E-01	1.68E+00	4.94E-01	1.07E+00	5.02E+00	3.43E-02	5.47E+00	1.87E-02	2.19E-02	3.91E+00

Table 6 (continued)

Fn.	D	MPSO	SDE	SBBO	ASMO	ISSA	MGOA	IBA	GSA	DGSA	OGSA	MGSA(I)	MGSA(II)	AGSA	LKGSA	CKGSA	EKGSA	IGSA
C_{17}	10	1.21E+01	4.23E+02	9.93E+00	1.36E+01	3.19E+01	6.58E+01	1.15E+01	5.46E+01	3.52E+01	1.50E+01	2.83E+01	3.64E+01	1.39E+01	3.83E+01	1.80E+01	1.43E+01	1.00E+01
	30	7.04E+01	7.75E+01	3.53E+01	7.54E+01	3.76E+02	3.88E+02	9.16E+02	6.74E+02	4.82E+02	8.38E+02	1.50E+02	2.41E+02	7.26E+01	4.73E+02	8.95E+01	6.73E+01	4.72E+01
	50	3.14E+02	2.83E+02	1.99E+02	6.98E+02	1.79E+03	1.11E+03	1.61E+03	1.16E+03	1.52E+03	8.62E+01	8.65E+02	9.13E+02	7.11E+02	1.80E+03	6.53E+02	7.35E+02	1.28E+02
	90	1.00E+03	7.69E+02	6.74E+02	2.10E+03	4.45E+03	2.53E+03	3.47E+03	2.71E+03	3.84E+03	4.12E+02	2.41E+03	2.47E+03	2.24E+03	5.35E+03	2.08E+03	2.15E+03	2.20E+02
C_{18}	10	2.94E+01	4.18E+02	2.75E+01	1.44E+01	3.25E+01	5.14E+01	3.98E+01	5.89E+01	3.19E+01	1.56E+01	3.61E+01	3.79E+01	1.32E+01	4.36E+01	1.84E+01	1.51E+01	2.95E+01
	30	2.73E+02	2.59E+02	1.43E+02	7.19E+01	3.32E+02	3.20E+02	9.58E+02	6.20E+02	5.36E+02	8.26E+02	2.18E+02	2.47E+02	6.57E+01	4.66E+02	8.41E+01	1.07E+02	4.66E+01
	50	6.49E+02	5.54E+02	4.54E+02	7.33E+02	1.97E+03	1.07E+03	1.61E+03	1.13E+03	1.44E+03	6.92E+02	9.28E+02	8.99E+02	7.35E+02	9.35E+01	6.52E+02	6.72E+02	2.13E+02
	90	1.50E+03	1.20E+03	1.03E+03	2.16E+03	4.40E+03	2.51E+03	3.44E+03	2.70E+03	3.56E+03	2.99E+03	2.48E+03	2.54E+03	2.22E+03	5.48E+03	2.67E+02	2.26E+03	3.58E+02
C_{19}	10	6.02E-01	3.77E+00	1.31E+00	1.46E+00	1.67E+00	1.39E+00	4.67E-01	3.46E+00	1.25E+00	1.41E+00	1.88E+00	2.02E+00	1.36E+00	2.40E+00	3.69E-01	7.75E-01	3.98E-01
	30	4.02E+00	8.12E+00	3.40E+00	7.59E+00	5.45E+01	9.92E+00	3.66E+05	5.87E+02	2.57E+01	3.07E+05	1.82E+01	1.90E+01	7.73E+00	5.60E+02	4.22E+00	5.96E+00	2.64E+00
	50	2.54E+01	2.98E+01	1.73E+01	1.19E+04	7.04E+05	2.95E+04	6.90E+05	1.42E+05	2.51E+04	1.93E+01	1.95E+04	8.12E+03	9.75E+03	2.09E+06	3.16E+02	2.06E+03	7.04E+00
	90	2.05E+02	1.08E+02	5.86E+01	2.66E+05	7.65E+06	3.59E+05	1.99E+06	9.99E+05	1.40E+06	8.54E+02	4.05E+05	3.14E+05	2.38E+05	1.30E+07	5.24E+04	1.18E+05	3.20E+01
C_{20}	10	3.12E+01	3.11E+02	3.24E+01	6.86E+01	6.88E+01	1.10E+02	3.88E+01	2.96E+01	4.81E+01	2.19E+01	2.58E+01	5.97E+01	1.02E+02	4.86E+01	1.37E+01	1.39E+01	1.01E+01
	30	4.39E+02	3.88E+02	2.25E+02	1.12E+03	8.46E+02	8.93E+02	6.98E+02	7.37E+02	9.14E+02	7.99E+02	1.02E+03	6.91E+02	5.25E+02	9.79E+02	9.04E+02	2.75E+02	2.49E+02
	50	4.28E+02	4.59E+02	2.70E+02	1.81E+03	5.57E+03	9.42E+02	1.10E+03	1.50E+03	1.38E+03	4.37E+02	1.87E+03	2.25E+03	1.65E+03	1.47E+03	1.48E+03	3.28E+02	2.93E+02
	90	1.00E+03	6.05E+02	9.08E+02	3.29E+03	1.12E+04	3.26E+03	4.79E+03	6.82E+03	3.78E+03	1.54E+03	5.66E+03	3.81E+03	1.75E+03	2.65E+03	5.28E+03	4.00E+03	4.59E+02

First Best value; Second Best value; Third Best value

Table 7 Comparative analysis of existing and new algorithms for mean fitness values over 30 runs on the CEC2013 benchmark functions ($C_{21} - C_{28}$) for considered dimensions

Fn.	D	MPSO	SDE	SBBO	ASMO	ISSA	MGOA	IBA	GSA	DGSA	OGSA	MGSA(I)	MGSA(II)	AGSA	LKGSA	CKGSA	EKGSA	IGSA
C_{21}	10	4.03E+02	4.11E+02	3.94E+02	3.85E+02	4.18E+02	4.29E+02	4.18E+02	4.40E+02	4.25E+02	4.62E+02	4.29E+02	3.74E+02	4.18E+02	4.49E+02	4.07E+02	4.43E+02	3.41E+02
	30	3.43E+02	2.55E+02	3.23E+02	3.59E+02	7.17E+02	3.59E+02	2.78E+03	1.63E+03	3.39E+02	2.75E+03	3.59E+02	4.45E+02	3.39E+02	1.69E+03	3.39E+02	2.94E+02	2.68E+02
	50	7.58E+02	9.63E+02	9.84E+02	3.52E+03	4.93E+03	3.70E+03	5.05E+03	4.18E+03	3.44E+03	1.01E+03	3.67E+03	3.40E+03	3.50E+03	7.12E+03	2.81E+03	3.22E+03	5.32E+02
	90	9.91E+02	3.92E+02	7.58E+02	5.13E+03	1.14E+05	5.39E+03	7.58E+03	6.67E+03	6.91E+03	7.66E+02	5.17E+03	5.27E+03	5.19E+03	1.48E+04	4.48E+03	4.92E+03	5.45E+02
C_{22}	10	2.01E+02	2.01E+03	4.75E+02	1.93E+03	2.24E+03	2.86E+03	5.52E+01	2.55E+03	1.07E+03	3.00E+02	1.90E+03	1.88E+03	1.86E+03	2.23E+03	1.98E+03	3.33E+02	1.14E+01
	30	9.17E+02	2.51E+03	1.80E+03	7.04E+03	7.67E+03	8.50E+03	9.01E+03	8.13E+03	4.04E+03	9.84E+03	6.82E+03	7.83E+03	7.00E+03	6.58E+03	6.66E+03	2.23E+03	1.61E+03
	50	4.52E+03	8.17E+03	5.51E+03	1.43E+04	1.62E+04	1.54E+04	1.80E+04	1.51E+04	1.07E+04	7.96E+03	1.45E+04	1.60E+04	1.42E+04	1.88E+04	1.84E+03	1.43E+04	3.91E+03
	90	1.51E+04	2.28E+04	1.46E+04	2.73E+04	3.12E+04	2.73E+04	3.35E+04	2.88E+04	2.49E+04	2.03E+04	2.77E+04	3.11E+04	2.65E+04	3.57E+04	2.64E+04	4.82E+03	5.09E+03
C_{23}	10	8.11E+02	1.93E+03	1.44E+03	1.31E+03	1.94E+03	2.23E+03	1.25E+03	2.18E+03	9.78E+02	1.85E+02	1.33E+03	1.40E+03	1.31E+03	1.85E+03	1.43E+03	7.38E+02	1.11E+03
	30	7.54E+03	8.62E+03	5.86E+03	6.33E+03	7.12E+03	6.95E+03	9.03E+03	7.71E+03	6.81E+03	9.92E+03	6.50E+03	7.24E+03	6.43E+03	7.37E+03	6.27E+03	3.76E+03	2.61E+03
	50	1.62E+04	1.68E+04	1.23E+04	1.35E+04	1.51E+04	1.40E+04	1.91E+04	1.52E+04	1.45E+04	9.74E+03	1.42E+04	1.55E+04	1.37E+04	1.90E+04	1.36E+04	1.37E+04	6.34E+03
	90	2.52E+04	2.92E+04	1.99E+04	2.57E+04	2.99E+04	2.55E+04	3.48E+04	2.80E+04	2.56E+04	1.82E+04	2.59E+04	2.97E+04	2.52E+04	3.53E+04	2.46E+04	2.50E+04	1.33E+04
C_{24}	10	2.29E+02	2.71E+02	2.38E+02	2.44E+02	1.95E+02	2.81E+02	2.34E+02	2.79E+02	2.36E+02	2.20E+02	2.46E+02	2.43E+02	2.37E+02	2.57E+02	2.45E+02	2.25E+02	1.92E+02
	30	2.99E+02	3.15E+02	2.89E+02	3.45E+02	5.14E+02	6.15E+02	6.78E+02	5.73E+02	3.60E+02	4.48E+02	3.82E+02	3.31E+02	3.81E+02	4.34E+02	3.85E+02	2.68E+02	2.00E+02
	50	3.83E+02	4.21E+02	3.36E+02	1.06E+03	2.45E+03	1.40E+03	1.24E+03	1.20E+03	4.97E+02	4.05E+02	8.86E+02	5.99E+02	1.02E+03	2.54E+02	9.02E+02	1.02E+03	2.91E+02

Table 7 (continued)

Fn.	D	MPSO	SDE	SBBO	ASMO	ISSA	MGOA	IBA	GSA	DGSA	OGSA	MGSA(I)	MGSA(II)	AGSA	LKGSA	CKGSA	EKGSA	IGSA
	90	4.88E+02	5.69E+02	4.29E+02	2.82E+03	4.47E+03	3.00E+03	3.35E+03	3.06E+03	1.16E+03	3.94E+02	2.84E+03	2.65E+03	2.76E+03	3.23E+03	2.55E+03	2.60E+03	3.53E+02
C_{25}	10	2.31E+02	2.62E+02	2.35E+02	2.32E+02	2.33E+02	2.70E+02	2.30E+02	2.70E+02	2.38E+02	2.20E+02	2.28E+02	2.29E+02	2.29E+02	2.53E+02	2.34E+02	2.23E+02	1.79E+02
	30	3.13E+02	3.22E+02	3.30E+02	4.25E+02	4.34E+02	4.76E+02	4.68E+02	4.80E+02	3.88E+02	4.52E+02	4.33E+02	4.24E+02	4.26E+02	4.45E+02	4.38E+02	2.82E+02	2.00E+02
	50	4.39E+02	4.39E+02	4.27E+02	7.33E+02	8.50E+02	7.65E+02	7.15E+02	7.43E+02	5.85E+02	3.72E+02	7.34E+02	6.93E+02	7.40E+02	7.49E+02	7.11E+02	7.32E+02	3.20E+02
	90	6.01E+02	6.05E+02	5.96E+02	1.36E+03	1.77E+03	1.40E+03	9.80E+02	1.43E+03	1.01E+03	5.91E+02	1.39E+03	1.40E+03	1.42E+03	1.47E+03	1.31E+03	1.22E+02	4.15E+02
C_{26}	10	2.42E+02	3.36E+02	2.03E+02	3.61E+02	4.38E+02	3.58E+02	2.06E+02	3.42E+02	2.12E+02	2.07E+02	2.83E+02	2.40E+02	3.05E+02	2.78E+02	3.32E+02	1.84E+02	1.44E+02
	30	3.47E+02	2.32E+02	3.15E+02	3.76E+02	4.30E+02	4.38E+02	5.14E+02	4.76E+02	3.89E+02	3.23E+02	3.92E+02	3.48E+02	3.92E+02	4.31E+02	4.23E+02	2.00E+02	2.77E+02
	50	4.64E+02	3.44E+02	4.55E+02	5.10E+02	1.98E+03	6.18E+02	7.08E+02	6.70E+02	4.99E+02	3.17E+02	5.22E+02	4.53E+02	4.19E+02	6.13E+02	4.03E+02	4.38E+02	3.18E+02
	90	5.60E+02	6.92E+02	5.24E+02	1.31E+03	1.41E+05	1.99E+03	3.20E+03	2.72E+03	7.31E+02	4.46E+02	1.69E+03	8.86E+02	9.86E+02	3.00E+03	1.57E+03	1.27E+03	4.39E+02
C_{27}	10	4.23E+02	8.75E+02	5.41E+02	4.51E+02	3.58E+02	3.74E+02	4.67E+02	4.51E+02	5.75E+02	4.32E+02	4.42E+02	4.66E+02	4.68E+02	5.71E+02	4.31E+02	3.17E+02	3.47E+02
	30	7.58E+02	1.07E+03	1.20E+03	1.13E+03	1.05E+03	1.01E+03	9.04E+02	9.81E+02	7.93E+02	1.08E+03	1.16E+03	1.20E+03	9.87E+02	1.09E+03	1.01E+03	9.38E+02	3.01E+02
	50	1.84E+03	2.37E+03	1.70E+03	2.88E+03	5.88E+03	3.73E+03	3.99E+03	3.76E+03	2.62E+03	1.83E+03	3.00E+03	2.76E+03	3.03E+03	3.55E+03	2.75E+03	2.86E+03	8.91E+02
	90	2.92E+03	3.96E+03	2.41E+03	7.04E+03	1.18E+04	9.51E+03	1.11E+04	1.01E+04	5.31E+03	5.06E+03	6.03E+03	5.89E+03	7.18E+03	1.06E+04	5.92E+03	1.33E+03	1.78E+03
C_{28}	10	3.27E+02	2.29E+03	4.30E+02	6.64E+02	6.54E+02	1.06E+03	3.19E+02	1.04E+03	4.35E+02	3.21E+02	5.47E+02	6.64E+02	6.85E+02	9.11E+02	7.83E+02	3.19E+02	1.93E+02
	30	3.19E+02	3.52E+02	9.87E+02	4.43E+03	5.84E+03	5.59E+03	8.08E+03	5.44E+03	3.26E+03	6.68E+03	4.60E+03	4.68E+03	4.56E+03	4.38E+03	4.80E+03	3.19E+02	2.22E+02
	50	1.50E+03	5.05E+02	4.25E+02	9.40E+03	4.69E+04	1.00E+04	1.38E+04	1.06E+04	6.75E+03	4.80E+02	9.68E+03	1.02E+04	9.60E+03	1.26E+04	8.83E+03	9.28E+03	6.75E+02
	90	2.41E+03	1.51E+03	1.34E+03	1.41E+04	2.78E+04	1.48E+04	2.09E+04	1.79E+04	1.63E+04	4.17E+03	1.43E+04	1.62E+04	1.43E+04	2.44E+04	1.36E+04	1.41E+04	3.93E+02

First Best value; Second Best value; Third Best value

5.1.1 Convergence analysis

As vindicated from the results, IGSA outperformed other algorithms om the majority of the functions with 30 dimensions. Therefore, the convergence analysis of IGSA has been performed on the three functions taken from each category namely Unimodal (F_9), Multimodal (F_5), and CEC2013 (C_2). The same is depicted in Fig. 4, where x-axis represents iteration number and vertical axis depicts the fitness value in logarithmic scale. It can be clearly seen from the convergence graph that IGSA converges smoothly by first exploring the search space followed by deeper exploitation in the later stage of the iterations. Thus, IGSA also validated its better convergence ability as compared to the other state-of-the-art methods.

5.2 Analysis of considered variants on Breast cancer nuclei segmentation

Now-a-days, triple negative breast cancer (TNBC) is one of the most critical types of breast cancer as it grows very fast. The chances of recurring are also very high. Histopathological image analysis plays a key role in medical domain for identification and analysis of the disease. Particularly, nuclei segmentation from these images may be used to detect cancerous cells for early diagnosis and prognosis of breast cancer. In this section, TNBC breast cancer dataset [45] has been used which is a publicly available dataset consisting of 50 histopathological images generated through scanning on 40× magnification level of tissue slides via Ultra fast scanner 1.6 RA. These tissues are stained with H&E staining. Due to staining and other morphological variations, the background of these images are very complex which make them very hard to analyze. Some of the images from the considered dataset is shown in Fig. 5.

In this paper, clustering-based approach is followed to segment the nuclei. To perform clustering, Kmeans and four meta-heuristic methods are considered, namely GSA, AGSA, EKGSA, and IGSA. In experimentation, histopathological images are converted into *Lab*

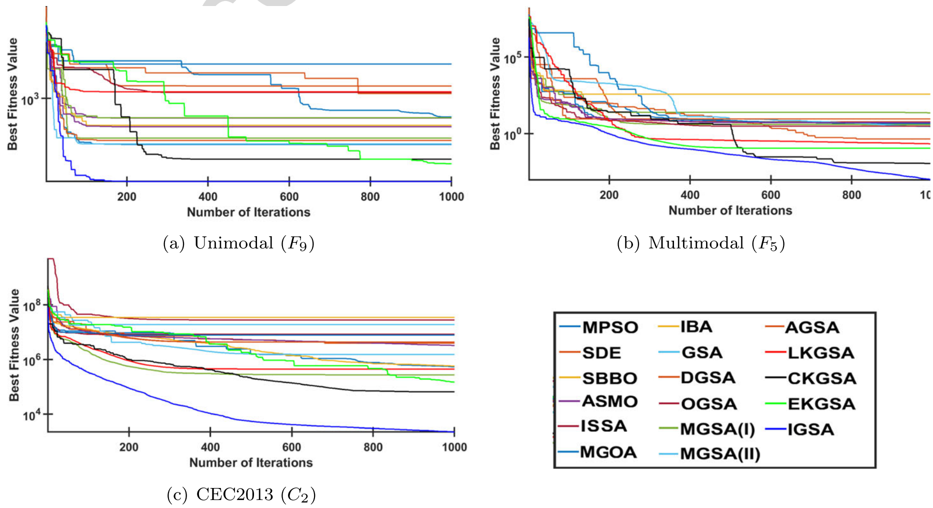

(a) Unimodal (F_9)

(b) Multimodal (F_5)

(c) CEC2013 (C_2)

Fig. 4 Convergence behavior of considered algorithms on representative benchmark functions over 30 dims

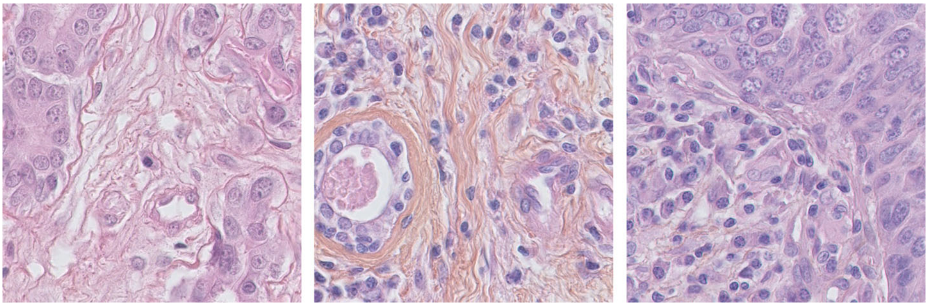

(a) (b) (c)

Fig. 5 Sample breast cancer histopathological images [45]

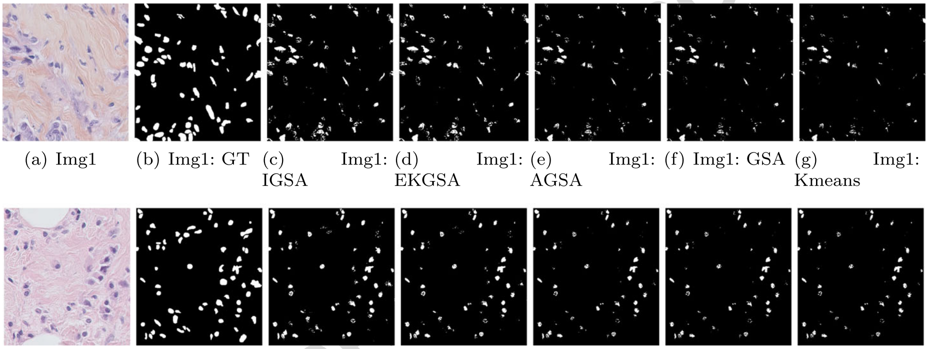

(a) Img1 (b) Img1: GT (c) Img1: IGSA (d) Img1: EKGSA (e) Img1: AGSA (f) Img1: GSA (g) Img1: Kmeans

(h) Img2 (i) Img2: GT (j) Img2: IGSA (k) Img2: EKGSA (l) Img2: AGSA (m) Img2: GSA (n) Img2: Kmeans

Fig. 6 Qualitative analysis of considered methods on four representative images taken from TNBC [45].

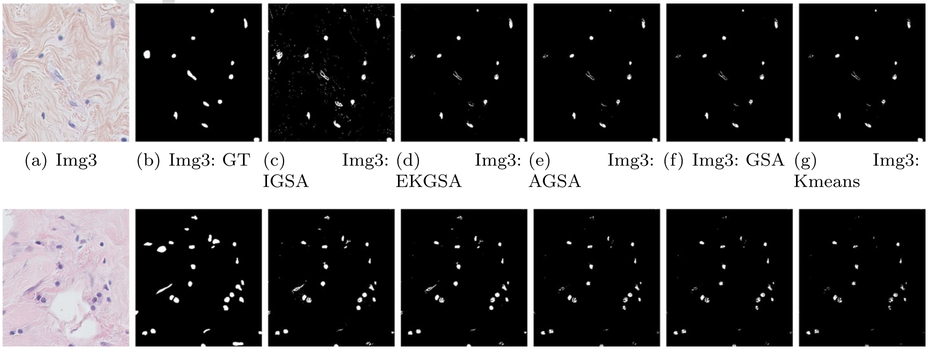

(a) Img3 (b) Img3: GT (c) Img3: IGSA (d) Img3: EKGSA (e) Img3: AGSA (f) Img3: GSA (g) Img3: Kmeans

(h) Img4 (i) Img4: GT (j) Img4: IGSA (k) Img4: EKGSA (l) Img4: AGSA (m) Img4: GSA (n) Img4: Kmeans

Fig. 7 Qualitative analysis of considered methods on four representative images taken from TNBC [45].

Table 8 Quantative analysis of considered methods in terms of aggregated jaccard index on representative images taken from TNBC [45]

Image	Kmeans	GSA	AGSA	EKGSA	IGSA
Image1	0.4838	0.4990	0.5150	0.5358	0.5535
Image2	0.5087	0.5236	0.5478	0.5785	0.5870
Image3	0.4234	0.4356	0.5419	0.5927	0.6126
Image4	0.4558	0.4686	0.5397	0.5404	0.5583
Image5	0.4745	0.4907	0.5146	0.5654	0.5838
Image6	0.2981	0.3069	0.5301	0.5708	0.5894
Image7	0.5303	0.5456	0.5890	0.5998	0.6198
Image8	0.2354	0.2420	0.5150	0.5358	0.5535
Avg. (100 Images)	0.4720	0.4851	0.5123	0.5430	0.5893

color space and clustering is performed on the values under 'a' and 'b' channels. The considered meta-heuristic method clusters the values into k optimal clusters. The cluster with minimum centroid value is considered as nuclei region in the segmented image [32].

The experiments are simulated on MATLAB 2017a with core i5 processor with 2.35 GHz and 16GB RAM. Figures 6 and 7 illustrate the nuclei segmentation results of the considered methods on four randomly selected images. For the quantative analysis of nuclei segmentation, the performance of considered meta-heuristic methods is compared in terms of aggregated Jaccard index (AJI). AJI is the quantitative measurement of segmentation accuracy. High value of AJI represent good segmentation. For $k = 5$, considered methods return best AJI value on the TNBC breast cancer images. The parameter settings of each method is kept according to respective literature. Table 8 depict the AJI values of each segmentation method on eight randomly selected images from TNBC breast cancer dataset along with the averaged AJI value obtained over the complete dataset. It can be observed that Kmeans-based and GSA-based segmentation methods did not attain averaged AJI value above 0.50. While, AGSA-based and EKGSA-based methods reported averaged AJI values as 0.51 and 0.54, respectively. This shows their average behavior in nuclei segmentation. Further, IGSA-based segmentation method performed better than other methods and returned 0.59 (approx.) which is highest value among all.

6 Conclusion

In this paper, ten variants that are modifying three parameters of gravitational search algorithm, namely position, velocity, and $Kbest$, have been presented. The variants try to improve the trade-off between the exploration and exploitation with the intention of better convergence trend and solution precision. In position-based variants, IGSA, DGSA, and OGSA have been considered while GGSA, MGSA(I), and MGSA(II) redefines the velocity equation. As $Kbest$ has linear decreasing value to control the exploration and exploitation trade-off of GSA,LKGSA, CKGSA, and EKGSA variants modify the $Kbest$.

The considered variants are validated by simulation results against seven recent meta-heuristic algorithms over two sets of benchmark functions belonging to the three types of problems, namely unimodal, multimodal, and real parameter single objective optimization problems of IEEE Congress on Evolutionary Computation (CEC), 2013. The experimental performance has been evaluated for four different functional dimensions i.e., 10, 30, 50, and 90 and studied in terms of mean fitness value, Friedman test, and convergence trend. It has been observed from the experimental and statistical results that IGSA has surpassed the considered algorithms over maximum number of benchmark problems in each dimension. The analysis of the convergence trends clearly indicates that the searching behavior of IGSA is better with consistency. Thus, it can be concluded that IGSA achieves better precision with balanced trade-off between exploration and exploitation.

Moreover, triple negative breast cancer (TNBC) dataset has been considered to analysis the performance of GSA variants for the nuclei segmentation. The considered TNBC dataset [45] is a publicly available dataset which consists of 50 histopathological images. Kmeans and four meta-heuristic methods, namely GSA, AGSA, EKGSA, and IGSA, have been considered and performance is analysed in terms of both qualitative and quantitive wherein aggregated Jaccard index (AJI) is used as performance measure. Experiments affirm that IGSA-based method performs better than other methods.

In future, the applicability of GSA variants on different complicated real-world problems defines a new prespective, especially problems related to big-data. The adaptability of different parameters of GSA still needs to be investigated in the perspective of convergence rate and trapping into local optima. Lastly, designing of new operators based on theories from physics related to gravity will advantage in leveraging the performance of GSA on different applications.

References

1. Bansal JC, Joshi SK, Nagar AK (2018) Fitness varying gravitational constant in gsa. Appl Intell 48(10):3446–3461
2. Brest J, Bošković B, Zamuda A, Fister I, Mezura-Montes E (2013) Real parameter single objective optimization using self-adaptive differential evolution algorithm with more strategies. In: Proc of IEEE congress on evolutionary computation, mexico, pp 377–383
3. Chatterjee A, Ghoshal S, Mukherjee V (2012) A maiden application of gravitational search algorithm with wavelet mutation for the solution of economic load dispatch problems. International Journal of Bio-Inspired Computation 4:33–46
4. Chaos theory and the logistic map - geoff boeing. http://geoffboeing.com/2015/03/chaos-theory-logistic-map/, (Accessed on 04/12/2016)
5. Davarynejad M, Forghany Z, van den Berg J (2012) Mass-dispersed gravitational search algorithm for gene regulatory network model parameter identification. In: Proc of springer asia-pacific conference on simulated evolution and learning, vietnam, pp 62–72
6. Dhal KG, Ray S, Das A, Das S (2018) A survey on nature-inspired optimization algorithms and their application in image enhancement domain. Archives of Computational Methods in Engineering, pp 1–32
7. Dixit M, Upadhyay N, Silakari S (2015) An exhaustive survey on nature inspired optimization algorithms. Int J Softw Eng Appl 9:91–104
8. Dorigo M, Birattari M, Stützle T (2006) Ant colony optimization. IEEE Comput Intell Mag 1:28–39
9. Feng Y, Teng G-F, Wang A-X, Yao Y-M (2007) Chaotic inertia weight in particle swarm optimization. In: Proc of IEEE international conference on innovative computing, information and control, japan, pp 475–480
10. Giladi C, Sintov A (2020) Manifold learning for efficient gravitational search algorithm. Inf Sci 517:18–36
11. Guha R, Ghosh M, Chakrabarti A, Sarkar R, Mirjalili S (2020) Introducing clustering based population in binary gravitational search algorithm for feature selection, Applied Soft Computing, pp 106341
12. Gupta V, Singh A, Sharma K, Mittal H (2018) A novel differential evolution test case optimisation (detco) technique for branch coverage fault detection. In: Smart Computing and Informatics, Springer, pp 245–254

13. Han X, Chang X (2012) A chaotic digital secure communication based on a modified gravitational search algorithm filter. Inf Sci 208:14–27
14. Ibrahim RA, Ewees AA, Oliva D, Abd Elaziz M, Lu S (2019) Improved salp swarm algorithm based on particle swarm optimization for feature selection. Journal of Ambient Intelligence and Humanized Computing 10(8):3155–3169
15. Jadon SS, Bansal JC, Tiwari R, Sharma H (2014) Artificial bee colony algorithm with global and local neighborhoods. International Journal of System Assurance Engineering and Management 9:1–13
16. Jiang J, Jiang R, Meng X, Li K (2020) Scgsa: A sine chaotic gravitational search algorithm for continuous optimization problems. Expert Syst Appl 144:113118
17. Kennedy J, Eberhart R (1995) Particle swarm optimization. In: IEEE Internation conference on neural networks
18. Khajehzadeh M, Taha MR, El-Shafie A, Eslami M (2012) A modified gravitational search algorithm for slope stability analysis. Eng Appl Artif Intell 25:1589–1597
19. Lei Z, Gao S, Gupta S, Cheng J, Yang G (2020) An aggregative learning gravitational search algorithm with self-adaptive gravitational constants Expert Systems with Applications, pp 113396
20. Li P, Duan H (2012) Path planning of unmanned aerial vehicle based on improved gravitational search algorithm. Sci China Technol Sci 55:2712–2719
21. Li C, Li H, Kou P (2014) Piecewise function based gravitational search algorithm and its application on parameter identification of avr system. Neurocomputing 124:139–148
22. Liu H, Wang Y, Tu L, Ding G, Hu Y (2018) A modified particle swarm optimization for large-scale numerical optimizations and engineering design problems. J Intell Manuf 29:1–27
23. Liu J, Xing Y, Ma Y, Li Y (2020) Gravitational search algorithm based on multiple adaptive constraint strategy. Computing, pp 1–41
24. Logistic map – from wolfram mathworld. http://mathworld.wolfram.com/LogisticMap.html, (Accessed on 04/16/2016)
25. Luo J, Chen H, Xu Y, Huang H, Zhao X et al (2018) An improved grasshopper optimization algorithm with application to financial stress prediction. Appl Math Model 64:654–668
26. Mirjalili S, Hashim SZM (2010) A new hybrid psogsa algorithm for function optimization. In: Proc of IEEE international conference on computer and information application, china, pp 374–377
27. Mirjalili S, Lewis A (2014) Adaptive gbest-guided gravitational search algorithm. Neural Comput Applic 25:1569–1584
28. Mittal H (2018) M. saraswat, ckgsa based fuzzy clustering method for image segmentation of rgb-d images. In: Proc of IEEE international conference on contemporary computing, India
29. Mittal H, Pal R, Kulhari A, Saraswat M (2016) Chaotic kbest gravitational search algorithm (ckgsa). In: Proc of IEEE international conference on contemporary computing, India
30. Mittal H, Saraswat M (2018) An optimum multi-level image thresholding segmentation using non-local means 2d histogram and exponential kbest gravitational search algorithm. Eng Appl Artif Intell 71:226–235
31. Mittal H, Saraswat M (2018) An image segmentation method using logarithmic kbest gravitational search algorithm based superpixel clustering. Evol Intel, pp 1–13
32. Mittal H, Saraswat M (2019) An automatic nuclei segmentation method using intelligent gravitational search algorithm based superpixel clustering. Swarm and Evolutionary Computation 45:15–32
33. Mittal H, Saraswat M (2019) Classification of histopathological images through bag-of-visual-words and gravitational search algorithm. In: Soft computing for problem solving, Springer
34. Mittal H, Saraswat M, Pal R (2020) Histopathological image classification by optimized neural network using igsa. In: International conference on distributed computing and internet technology, Springer, pp 429–436
35. Mukherjee M, Mitra S, Acharyya S (2020) Mutation-based chaotic gravitational search algorithm. In: Proceedings of the global AI congress 2019, Springer, pp 117–131
36. Nagaraju S, Reddy AS, Vaisakh K (2019) Shuffled differential evolution-based combined heat and power economic dispatch. In: Proc of springer international conference on soft computing in data analytics, singapore, pp 525–532
37. Nanda SJ, Panda G (2014) A survey on nature inspired metaheuristic algorithms for partitional clustering. Swarm and Evolutionary Computation 16:1–18
38. Nayyar A, Garg S, Gupta D, Khanna A (2018) Evolutionary computation: theory and algorithms. In: advances in swarm intelligence for optimizing problems in computer science, Chapman and Hall/CRC, pp 1–26
39. Nayyar A, Le D-N, Nguyen NG (2018) Advances in swarm intelligence for optimizing problems in computer science. CRC Press

40. Nayyar A, Nguyen NG (2018) Introduction to swarm intelligence. Advances in Swarm Intelligence for Optimizing Problems in Computer Science, pp 53–78
41. Niknam T, Golestaneh F, Malekpour A (2012) Probabilistic energy and operation management of a microgrid containing wind/photovoltaic/fuel cell generation and energy storage devices based on point estimate method and self-adaptive gravitational search algorithm. Energy 43:427–437
42. Olivas F, Valdez F, Melin P, Sombra A, Castillo O (2019) Interval type-2 fuzzy logic for dynamic parameter adaptation in a modified gravitational search algorithm. Inf Sci 476:159–175
43. Pal R, Saraswat M (2019) Histopathological image classification using enhanced bag-of-feature with spiral biogeography-based optimization. Appl Intell, pp 1–19
44. Pelusi D, Mascella R, Tallini L, Nayak J, Naik B, Deng Y (2020) Improving exploration and exploitation via a hyperbolic gravitational search algorithm. Knowl-Based Syst 193:105404
45. Peterjacknaylor/drfns This repository contains the code necessary in order to reproduce the work contained in the submitted paper: segmentation of nuclei in histopathology images by deep regression of the distance map. https://github.com/PeterJackNaylor/DRFNS, (Accessed on 08/06/2020)
46. Rashedi E, Nezamabadi-Pour H, Saryazdi S (2009) Gsa: a gravitational search algorithm. Inf Sci 179:2232–2248
47. Rashedi E, Nezamabadi-Pour H, Saryazdi S (2009) Gsa: a gravitational search algorithm. Inf Sci 179:2232–2248
48. Rashedi E, Rashedi E, Nezamabadi-pour H (2018) A comprehensive survey on gravitational search algorithm. Swarm and Evolutionary Computation 41:141–158
49. Rawal P, Sharma H, Sharma N (2020) Fast convergent gravitational search algorithm. In: Recent trends in communication and intelligent systems, Springer, pp 1–12
50. Sabri NM, Puteh M, Mahmood MR (2013) A review of gravitational search algorithm. International Journal of Advances in Soft Computing and its Application 5:1–39
51. Sarafrazi S, Nezamabadi-Pour H, Saryazdi S (2011) Disruption: a new operator in gravitational search algorithm. Scientia Iranica 18:539–548
52. Sharma A, Sharma A, Panigrahi BK, Kiran D, Kumar R (2016) Ageist spider monkey optimization algorithm. Swarm and Evolutionary Computation 28:58–77
53. Shaw B, Mukherjee V, Ghoshal S (2012) A novel opposition-based gravitational search algorithm for combined economic and emission dispatch problems of power systems. International Journal of Electrical Power & Energy Systems 35:21–33
54. Simon D (2008) Biogeography-based optimization. IEEE Trans Evol Comput 12:702–713
55. Storn R, Price K (1997) Differential evolution–a simple and efficient heuristic for global optimization over continuous spaces. J Glob Optim 11:341–359
56. Tan Z, Zhang D (2020) A fuzzy adaptive gravitational search algorithm for two-dimensional multilevel thresholding image segmentation. Journal of Ambient Intelligence and Humanized Computing, pp 1–12
57. Thakur AS, Biswas T, Kuila P Binary quantum-inspired gravitational search algorithm-based multi-criteria scheduling for multi-processor computing systems, JOURNAL OF SUPERCOMPUTING
58. Tsai H-C, Tyan Y-Y, Wu Y-W, Lin Y-H (2013) Gravitational particle swarm. Appl Math Comput 219:9106–9117
59. Wang M, Wan Y, Ye Z, Gao X, Lai X (2018) A band selection method for airborne hyperspectral image based on chaotic binary coded gravitational search algorithm. Neurocomputing 273:57–67
60. Wang Y, Yu Y, Gao S, Pan H, Yang G (2019) A hierarchical gravitational search algorithm with an effective gravitational constant. Swarm and Evolutionary Computation 46:118–139
61. Whitley D (1994) A genetic algorithm tutorial. Statistics and computing 4:65–85
62. Wu Z, Yu D (2018) Application of improved bat algorithm for solar pv maximum power point tracking under partially shaded condition. Appl Soft Comput 62:101–109
63. Yin B, Guo Z, Liang Z, Yue X (2018) Improved gravitational search algorithm with crossover. Computers & Electrical Engineering 66:505–516

Publisher's note Springer Nature remains neutral with regard to jurisdictional claims in published maps and institutional affiliations.

AUTHOR QUERY

AUTHOR PLEASE ANSWER QUERY:

Q1. All authors were affiliated tot he same affiliation. PLease confirm if correct. Otherwise, please provide correct affiliations of all authors.